American Mineralogist, Volume 67, Pages 421–450, 1982

Molecules as models for bonding in silicates[1]

G. V. GIBBS

Department of Geological Sciences
Virginia Polytechnic Institute and State University
Blacksburg, Virginia 24061

Abstract

Computational quantum chemistry is a powerful method developed by the chemist to elucidate bond length and angle variations, electron density distributions, spectra, reactions and energetics of small molecules. Because little difference exists between the shapes and sizes of SiOSi groups in gas phase siloxane molecules and solid silicates, the method has been employed to generate potential energy surfaces and deformation maps for a variety of molecules especially designed to model the bonding properties of complex silicate minerals. The use of computational quantum chemistry in studying the chemical bonding in these minerals is motivated by a need to understand the physical laws that govern their structures and stabilities beyond that afforded by Pauling's rules. The ability of this *ab initio* method to mimic *a priori* bond length and angle variations, charge density distributions and force constants of silicates and other solids indicates that these observables are governed in large part by the local atomic arrangement.

A survey of these computations shows that the quantum mechanically derived SiO bond lengths for hydroxyacid molecules and 4- and 6-coordinate Si are in good agreement with those in comparable silicates. Also, theoretical and experimental deformation maps of these bonds show modest accumulations of charge density between Si and O in conformity with the partial covalent character of the SiO bond. Potential energy curves generated for the molecules $H_6Si_2O_7$, $H_6SiAlO_7^{1-}$, $H_6SiBO_7^{1-}$ and $H_6SiBeO_7^{2-}$ yield equilibrium bridging bond lengths and angles in close agreement with those in silicates with SiOT (T=Si,Al,B,Be) groups. The relatively narrow range of angles exhibited by the SiOB and SiOBe groups and the wide range of angles exhibited by SiOSi and SiOAl groups conform with the shape of each curve. Bond lengths calculated for hydroxyacid molecules containing first and second period metal atoms are linearly correlated with coordination number as observed in studies of crystal radii. By reproducing the bond strength versus bond length trends and the correlation between bond strength sum and bond length, the calculations have provided a quantum mechanical underpinning of Pauling's electrostatic valence rule. The assertion that the electrostatic bond strength, s, can be equated with bond number is corroborated by a strong correlation between s and bond overlap population. In addition to providing a good account of bond length and angle variations in silicates, thiosilicates and aminosilicates, the calculations have also afforded valuable insights into the compressibilities, the polymorphism and the glass forming tendencies of silica. The achievements of the calculations examined in this survey indicate that computational quantum chemistry is destined to become an important tool in mineralogy for identifying systematic relationships between structural and physical properties and for furnishing new insights into the many types of reactions involving minerals.

Introduction

Since the development in the early sixties of modern single crystal diffractometers, gas phase electron diffraction apparatus and high speed digital computers, the structures of a large number of silicates and gas phase and molecular crystal siloxanes have appeared in the literature, providing a wealth of accurate bond length and angle data. One of the most important results afforded by these data has been the discovery that very little difference

[1] Presidential Address, Mineralogical Society of America. Delivered at the 62nd Annual Meeting of the Society, November 3, 1981.

0003–004X/82/0506–0421$02.00

exists between the size and shape of a disiloxy (SiOSi) group in a solid silicate and in a siloxane molecule (Table 1). For example, the disiloxy group in the silicate α-quartz has an angle of 144° and a SiO bond length of 1.61Å which is in close agreement with an angle of 144° and a bond length of 1.63Å in the gas phase molecule disiloxane $(H_3Si)_2O$ (Almenningen, Bastiansen, Ewing, Hedberg and Traetteberg, 1963; Gibbs, Hamil, Louisnathan, Bartell and Yow, 1972; Tossell and Gibbs, 1978; Barrow, Ebsworth and Harding, 1979; Gibbs, Meagher, Newton and Swanson, 1981). Despite the intermolecular forces, crystallization of this gas phase molecule into a molecular solid has virtually no effect on the shape of the group (Table 1). Thus, as observed by Barrow *et al.* (1979), the packing of the molecule in the solid seems to conform with the shape of the group in the free molecule rather than *vice versa*. Also, Table 1 shows that the shape of the group is virtually the same, on the average, as that in solid siloxanes, silicates and silica glass. Thus, the forces that control the size and shape of the disiloxy group in disiloxane and in α-quartz as well as other silicates seem to be nearly the same, notwithstanding the absence in the gas phase molecule of the long range Madelung potential peculiar to a solid. Thus, on the one hand, a mineral like α-quartz can be portrayed as a molecule of megascopic dimensions held together by essentially the same forces that hold the SiOSi group together in the molecule. On the other hand, disiloxane can be portrayed as a tiny hydrogenated SiOSi moiety of the α-quartz structure. Because of the relatively small size of the molecule, computational quantum chemistry can be used to evaluate its wave functions and to probe the properties of its disiloxy group (Newton and Gibbs, 1979, 1980; Newton, 1981; Sauer and Zurawski, 1979; Meier and Ha, 1980; Oberhammer and Boggs, 1980; Ernst, Allred, Ratner, Newton, Gibbs, Moskowitz and Topiol, 1981). Moreover, because the bonding in the molecule appears to be similar to that in α-quartz, we might expect that molecular orbital (MO) calculations on small molecules with SiOSi groups can be applied to the groups in α-quartz thereby improving our understanding of the length and stiffness of its SiO bond, the energetics and compliance of its SiOSi angle, its isothermal bulk modulus, and its electron density distribution (Newton and Gibbs, 1980; Newton, O'Keeffe and Gibbs, 1980; Gibbs *et al.*, 1981).

Table 1: Comparison of experimental bond lengths, R(SiO), and angles for the SiOSi groups in gas phase and solid state molecular crystal siloxanes and silicates.

	R(SiO)Å	∠SiOSi(°)	Reference
$(H_3Si)_2O$ (gas)	1.63	144	Almenningen et al. (1963)
$(H_3Si)_2O$ (solid)	1.63	142	Barrow et al. (1979)
Siloxanes (solid)[a]	1.63	140	Newton and Gibbs (1980)
Silicates (solid)[a]	1.63	145	Geisinger and Gibbs (1981b)
Silica glass[a]	1.62	152	Da Silva et al. (1975)

[a] Averaged values.

Since 1979 computational quantum chemistry has been used to generate potential energy surfaces for a variety of siloxane and silicate molecules especially designed to model the bonding in a number of solid silicates. The equilibrium geometries and energetics provided by these surfaces are in accord with the experimental geometries and force constants recorded for a number of solid state silicates, thiosilicates and aminosilicates (Newton and Gibbs, 1979, 1980; Meagher, Swanson and Gibbs, 1980; Swanson, Meagher and Gibbs, 1980; Downs and Gibbs, 1981; Geisinger and Gibbs, 1981a; Nakajima, Swanson and Gibbs, 1980). In addition, deformation electron density maps generated for the SiO bonds in molecules with one-, four- and six-coordinate Si are in qualitative agreement with experimental deformation distributions recently obtained for a number of silicates (Hill, Newton and Gibbs, 1981; Downs, Hill, Newton, Tossell and Gibbs, 1982; Stewart, in prep.; Newton and Gibbs, in prep.). Additional calculations have been completed in collaboration with Dr. R. J. Hill, CSIRO, Division of Mineral Chemistry, Port Melbourne, Australia, Professor E. P. Meagher of the Department of Geological Sciences at the University of British Columbia, Dr. M. D. Newton of the Chemistry Department at the Brookhaven National Laboratory, Professor Michael O'Keeffe of the Department of Chemistry at Arizona State University, Professor J. A. Tossell of the Department of Chemistry, University of Maryland (Gupta, Swanson, Tossell and Gibbs, 1980), and with my talented and bright students B. C. Chakoumakos, J. W. Downs, K. L. Geisinger, R. C. Peterson and D. K. Swanson (Chakoumakos, 1981; Chakoumakos and Gibbs, 1981a; Downs, 1980; Swanson, 1980; Peterson, 1980). The objective of this report is to examine, compare and summarize the results of these many calculations.

This paper is divided into five sections. In the

first section, the essentials of molecular orbital theory will be examined as it is used to estimate the total energy of a closed-shell molecule, to construct molecular potential energy surfaces, and to optimize molecular geometries. This will be followed by a discussion of Gaussian-type basis functions and their use in simplifying the two-electron integrals. Mulliken's recipe for calculating bond overlap populations will then be reviewed and related to the total electron density of the molecule. In the second section, molecular-orbital-generated geometries and deformation maps of the SiO bonds in silicate molecules with four- and six-coordinate Si will be compared to experimental bond lengths and deformation maps reported for solid silicates. Next, the contribution of the *d*-type polarization functions of Si to the wavefunctions of the molecules will be discussed. The third section of the report examines the geometry and force constants of the disiloxy group in the silica polymorphs in terms of a potential energy surface generated for the group in the disilicic acid molecule. It also compares static deformation maps of the SiOSi groups in α-quartz, disiloxane and silicon monoxide. The fourth section discusses the bridging bond lengths and angles reported for a number of silicates in terms of potential energy curves calculated on molecules with SiOSi, SiOAl, SiOB and SiOBe groups. The stiffness of the bridging angle in the thiosilicates and their limited assortment of tetrahedral topologies compared to those of silicates will next be discussed in terms of a potential energy curve generated for the disilathia (SiSSi) group. Then multiple linear regression methods will be employed to estimate the dependence of SiO and AlO bond length variations on the bond strength sum and the fractional *s*-character of the bridging oxygen. In the fifth section of the report, bond strength versus bond length curves generated with molecular orbital theory for hydroxyacid molecules containing first and second row atoms will be compared to empirical ones reported by Brown and Shannon (1973), and the electrostatic strengths of the bonds in the molecules will be correlated with the Mulliken bond overlap populations provided by the calculations.

Computational quantum chemistry

The molecular orbital method

In the last decade, computational quantum chemistry (Pople, 1973) has become an important tool for determining the structure and electron density distributions of a molecule and for providing insight into why molecules have their characteristic sizes, shapes and topologies. In addition, the method is amenable to simple interpretative algorithms that allow the information content of the total wavefunction to be distilled into a relatively small number of chemically informative quantities such as orbital and bond-overlap populations, atomic charges and deformation densities (Newton, 1981).

In the theory of molecular orbitals, the total wave function of a closed-shell molecule, ψ, is approximated by an antisymmetrized product of one-electron wavefunctions or molecular orbitals, ϕ_i,

$$\psi \approx \frac{1}{\sqrt{n!}} A \prod_{i=1}^{n} \phi_i \qquad (1)$$

where n is the total number of electrons in the molecule and A_i is the antisymmetrization operator. If ψ is normalized, then the total energy of the molecule, E_{mol}, is the expectation value of the Schrodinger Hamiltonian

$$E_{mol} = \int \psi^* H \psi d\tau \,, \qquad (2)$$

where H is the many-electron Hamiltonian operator which, if the nuclear kinetic energy terms are neglected, is the sum of the kinetic energy operators for the electrons together with the various Coulombic contributions to the potential energy. Minimization of the energy using the method of undetermined Lagrangian multipliers results in the effective one-electron Hartree-Fock equation:

$$F\phi_i = \varepsilon_i \phi_i \,, \qquad (3)$$

where F is the effective one-electron Hartree-Fock Hamiltonian operator for an electron in the environment of the molecule, and ε_i is the one-electron energy.

Since atoms are the building blocks for molecules, equation (3) may be solved approximately by constructing each molecular orbital as a linear combination of m atomic orbital (AO) basis functions, χ_ν, each centered on the atoms of the molecule,

$$\phi_i \approx \sum_{\nu=1}^{m} \chi_\nu C_{\nu i} \,, \qquad (4)$$

where $C_{\nu i}$ are the appropriate linear weighting coefficients.

If we substitute Eq. (4) into equation (3), multiply on the left by χ_μ and integrate, we obtain the

Roothaan equations for a closed-shell molecule (see Roothaan (1951), Parr (1964), Pople and Beveridge (1970) and Dewar (1969) for a more rigorous and informative derivation):

$$\sum_{\nu=1}^{m} (F_{\mu\nu} - \varepsilon_i S_{\mu\nu})C_{\nu i} = 0 , \qquad (5)$$

where ε_i are the orbital energies, $S_{\mu\nu}$ are the overlap integrals,

$$S_{\mu\nu} = \int \chi_\mu(1)\chi_\nu(1)d\tau_1 , \qquad (6)$$

where $d\tau_1$ is the volume element of electron 1 and

$$F_{\mu\nu} = H_{\mu\nu} + \sum_{\lambda\sigma} P_{\lambda\sigma}\left[(\mu\nu|\lambda\sigma) - \frac{1}{2}(\mu\lambda|\nu\sigma)\right] \qquad (7)$$

where

$$H_{\mu\nu} = \int \chi_\mu(1)\left\{-\frac{1}{2}\nabla_1^2 - \sum_A \frac{Z_A}{r_{1_A}}\right\}\chi_\nu(1)d\tau_1 , \qquad (8)$$

$$P_{\lambda\sigma} = 2\sum_i^{occ} C_{\lambda i}C_{\sigma i} , \qquad (9)$$

and

$$(\mu\nu|\lambda\sigma) = \iint \chi_\mu(1)\chi_\nu(1)1/r_{12}\chi_\lambda(2)\chi_\sigma(2)d\tau_1 d\tau_2 \qquad (10)$$

Subscripts μ, ν, λ and σ refer to basis functions, the symbols $\chi_\mu(1)$ and $\chi_\lambda(2)$ imply, for example, that electrons 1 and 2 are in atomic orbitals χ_μ and χ_λ, respectively, ∇^2 is the Laplacian operator, Z_A is the charge on the nucleus A and r_{pq} is the separation between particles p and q. The two-electron integrals defined in Eq. (10) represent electron interactions between orbital products $\chi_\mu\chi_\nu$ (1) and $\chi_\lambda\chi_\sigma$ (2), $H_{\mu\nu}$ represents the kinetic energy and the potential energy of attraction to the nuclear field of the orbital product $\chi_\mu\chi_\nu$ (1) and $P_{\lambda\sigma}$ is the density matrix element involving the coefficient products of the AO's χ_λ and χ_σ summed over each of the occupied molecular orbitals, ϕ_i.

Since each element of the Fock Matrix, $F_{\mu\nu}$, is dependent upon $P_{\lambda\sigma}$, equation (5) cannot be solved directly. In the absence of such a solution, an iterative procedure is usually adopted. For example, a minimum basis Huckel-type calculation will be performed to provide an initial set of density matrix elements and then the appropriate atomic integrals are accurately evaluated. With these results, the $F_{\mu\nu}$ elements of the Fock matrix and the $S_{\mu\nu}$ elements of the overlap matrix are constructed to formulate an m × m determinantal equation

$$|F_{\mu\nu} - \varepsilon_i S_{\mu\nu}| = 0 , \qquad (11)$$

which may be solved for m values of ε_i. Each new value of ε_i is then substituted in succession into equation (5) to give m new sets of coefficients, one set for each ε_i. The coefficients of the occupied MO's are next normalized and used to generate a new density matrix which in turn is used to compute a new Fock matrix and a new secular determinant whose non-trivial solutions yield an improved set of ε_i values. The procedure is repeated over and over again, each time starting with the results of the previous calculation until the elements of the density matrix converge to a final set of steady values that do not differ by some threshold value ($\sim 10^{-6}$) and self-consistency is obtained. This gives the "best set" of MO's from which the molecule's total energy can be estimated. When the MO's are written in LCAO form (Eq. 4), then the total SCF (self consistent field) electronic energy can be written as (Pople, 1953):

$$E_{el} = \frac{1}{2}\sum_{\mu\nu} P_{\mu\nu}(H_{\mu\nu} + F_{\mu\nu}) . \qquad (12)$$

Finally, an estimate of the molecule's total energy is found by adding the repulsion energy, $\Sigma_{A>B} Z_A Z_B/r_{AB}$, between the clamped nuclei of the molecule to equation 12.

Gaussian expansions of Slater type atomic orbitals

In the types of calculations described in this report, the expansion in equation (4) generally involves at least one basis function for each AO up to and including the valence shell on each atom in the molecule. Such a basis set is called a minimum basis set. For example, the minimum basis set for the molecule $H_6Si_2O_7$ would be the hydrogen 1*s* atomic function plus the silicon 1*s*, 2*s*, 2*p*, 3*s* and 3*p* functions and the oxygen 1*s*, 2*s* and 2*p* functions. As the size of the basis set is increased, the modeling of each molecular orbital improves and the SCF total energy becomes progressively lower. In the Hartree-Fock limit, where in principle an infinite number of basis set functions is required, the modeling of the MO's can neither be improved nor can the SCF energy be lowered further. Because the

number of terms in each LCAO must necessarily be finite for a large molecule like $H_6Si_2O_7$, it is important that rapidly convergent basis functions be used in the calculations. As Slater-type orbitals (STO) seem to best satisfy this requirement, ϕ_i in equation (4) is often expanded as a finite sum of STO's (functions with exponential dependence $\exp(-\zeta r)$). But, on the other hand, the two-electron integrals in equation (7) are extremely difficult and time consuming to evaluate when STO's are used as basis functions. This is particularly true when these integrals range over three or four atomic centers. A simplification found to alleviate this difficulty is to expand each STO as a sum of least-squares fitted primitive Gaussian functions (functions with exponential dependence $\exp(-\alpha r^2)$). Since the product of two Gaussian functions is itself a Gaussian function on line between the two functions (Boys, 1950; Shavitt, 1963), each four-centered integral, for example, may be replaced by a representative two-centered integral which may be rapidly evaluated with the computer. Thus, it is common practice in molecular orbital calculations to use a least-squares fitted combination of Gaussian functions (usually up to six) to mimic each Slater-type orbital, thereby speeding up the time of the calculation considerably (Hehre, Stewart and Pople, 1969; Binkley, Whiteside, Hariharan, Seeger, Hehre, Lathan, Newton, Ditchfield and Pople, 1978). As might be expected, the larger the number of primitive Gaussians used in the linear combination, the better we can mimic each STO, but, as might also be expected, the larger the expense of the increased computer storage. Thus, a trade-off must be made between the two, depending on the available funds, the quality of the trends sought, and the size of the molecule.

In this report, STO-3G and STO-3G* basis sets were employed to calculate the bond lengths and angles of the molecules studied. In the case of the STO-3G basis set, each occupied atomic orbital is represented by a single STO basis function which in turn is approximated by a sum of three primitive Gaussian functions. Hence, the abbreviation, STO-3G is used. On the other hand, when a manifold of five 3*d*-type polarization functions (each approximated by an individual primitive Gaussian function) is added to the STO-3G basis set of Si, the resulting basis is denoted as a STO-3G* basis (Collins, Schleyer, Binkley and Pople, 1976). Thus, by convention, the addition of a star to the abbreviation implies that the basis has been augmented by *d*-type wave functions.

The so-called "split valence" 66-31G* basis was used to calculate the bond lengths and angles and deformation density maps of the disiloxy group in disiloxane and deformation maps of the SiO bonds in the molecules H_4SiO_4 and H_8SiO_6. The K and L shell electrons in this basis are each represented by a minimal basis (represented by a combination of six Gaussian functions each) while the valence electrons are each represented by a double set of AO's (approximated by a sum of three Gaussians plus an additional Gaussian). The 3*d* AO's added to the *sp* basis of Si serve as polarization functions and appear to be necessary to mimic experimental deformation density distributions for the SiO bond (Newton and Gibbs, 1979).

Calculated molecular properties

The atomic nuclei and electrons comprising the atoms of a molecule strive to adopt a configuration wherein the total energy of the resulting structure is minimized.[2] By applying the principles of computational quantum chemistry, the energy of this structure can be estimated regardless of the type of bonding forces (ionic or covalent) that obtains between the constituent atoms. The optimized geometries of the molecules described in this report were found by minimizing the molecule's total energy by systematically adjusting the bond lengths and angles among the constituent atoms. In addition to optimizing the geometry, the topography of the resulting energy surface can provide considerable insight into a molecule's force constants as well as the expected variability of the molecule's bond lengths and angles. Further, a meaningful explanation of the bonding characteristics and charge distributions of the molecule can be obtained from a population analysis whereby the total number of electrons in the molecule is partitioned into the various atomic and bond contributions which are used to estimate atomic charges, bond overlap populations and deformation density distributions.

According to Mulliken (1955), the total molecular orbital electron density,

$$\rho(\mathbf{r}) = \sum_{i=1}^{n} \phi_i^*(\mathbf{r})\phi_i(\mathbf{r}), \qquad (13)$$

of a molecule can be expanded in terms of the AO

[2] Strictly speaking, this is true only at 0°K, but the effects of entropy, the TS term, are generally negligible compared to the total binding energy at all temperatures of geologic interest.

basis as

$$\rho(\mathbf{r}) = \sum_{\mu,\nu}^{m} P_{\mu\nu}\chi_{\mu}^{*}(\mathbf{r})\chi_{\nu}(\mathbf{r}), \qquad (14)$$

which when integrated over all space yields the total number of electrons:

$$n = \sum_{\mu,\nu}^{m} P_{\mu\nu}S_{\mu\nu} . \qquad (15)$$

The bond overlap population between the μ,ν pair of atomic orbitals is defined by

$$n(\mu\nu) = 2P_{\mu\nu}S_{\mu\nu} , \qquad (16)$$

which when summed over all the μ atomic orbitals on center M and all the ν atomic orbitals on center N, is defined as the bond overlap population n(MN) for the atom pair MN. As discussed by Mulliken (1932, 1935) in his original formulation, a positive or negative value for n(MN) corresponds to net bonding (attraction) or antibonding (repulsion) between atoms M and N.

For the calculations presented in this report, the Gaussian 76 computer program (Binkley *et al.*, 1978) was employed to calculate the Fock and overlap matrix elements and to solve the appropriate equations as discussed above to obtain the linear coefficients for the best set of molecular orbitals and an estimate of the total energy of the molecule as well as other molecular properties (Schaefer, 1977; Carsky and Urban, 1980).

The SiO bond

Tetrahedral silicate group

The most important structural moiety in many silicates is the tetrahedral silicate group. The SiO bond in this group is observed in silicates to range in length from 1.55 to 1.76Å with a mean value of 1.626Å, while the SiO bond in the silanol (SiOH) group in four-coordinate $SiO_3(OH)^{3-}$ and $SiO_2(OH)_2^{2-}$ groups in hydrated silicates shows a smaller range in lengths from 1.63 to 1.70Å with a somewhat larger mean value of 1.67Å (Gibbs *et al.*, 1981).

The monosilicic acid molecule, $Si(OH)_4$, is of particular interest in that it is the simplest entity to contain the silicate tetrahedral group. Although the molecule occurs in almost all aqueous environments on earth, it polymerizes spontaneously when concentrated in amounts greater than about the solubility of amorphous silica (~115 ppm SiO_2 at 25°C) and hence has never been isolated for a structural analysis (Iler, 1979). As computational quantum chemistry has become a standard method for determining molecular structure, Newton and Gibbs (1980) and Gibbs *et al.* (1981) undertook structural analyses of the molecule using molecular orbital STO-3G and Pulay (1969) gradient methods. Assuming that the topology of the molecule involves a silicon atom bonded to four hydroxyl groups, the structural analyses indicate the molecule to possess S_4 ($=\bar{4}$) point symmetry with four SiO bond lengths of 1.65Å, four OSiO angles of 107.1°, two of 114.2°, four OH bonds of 0.98Å and four SiOH angles of 108.8° (Fig. 1). Not only is this geometry in close agreement with that of silicate groups in the monosilicates (Fig. 2) and in hydrated silicates, but also the fundamental breathing frequency (8.14 m^{-1}) calculated from the SiO stretching force constant (665 Nm^{-1}) of the molecule agrees with that observed (8.19 m^{-1}) for tetrahedral silicate groups in aqueous solution (Gibbs *et al.*, 1981).

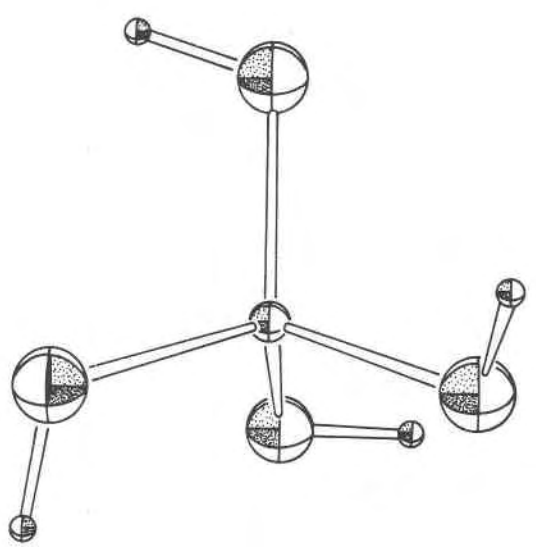

Fig. 1. A drawing of the molecular structure of monosilicic acid, H_4SiO_4, as determined by molecular orbital methods. The intermediate-sized sphere at the center of the molecule represents a silicon atom, and the four large spheres disposed at the corners of a tetrahedron and attached to Si represent oxygen atoms. The small sphere attached to each oxygen atom represents hydrogen. No significance is attached to the relative sizes of the spheres. (After Gibbs *et al.*, 1981.)

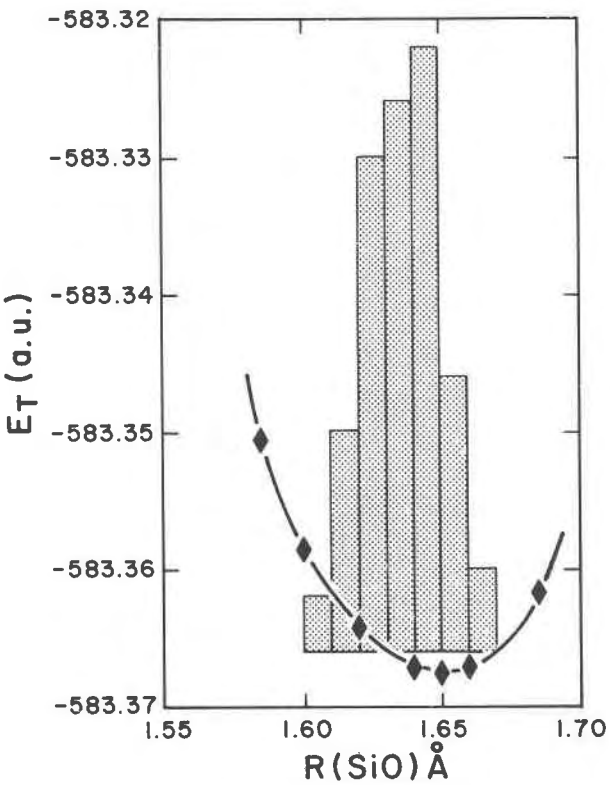

Fig. 2. The total energy, E_T, of the monosilicic acid molecule (S_4 point symmetry) calculated as a function of its SiO bond length, R(SiO). Data used to prepare this plot were taken from Table 1 of Newton and Gibbs (1980). The histogram superimposed on the plot is a frequency distribution of the experimental SiO bond lengths in the monosilicates. The average bond length for this group of minerals is 1.635Å compared with a minimum value of 1.65Å. E_T is given in atomic units (a.u.) where 1 a.u. = 6.275×10^2 kcal mole^{-1}.

Si3d orbital population

More than forty years have passed since Pauling (1939) made the controversial proposal that silicon may utilize its relatively unstable 3*d*-orbitals in forming double bonds with the oxygen atoms of a silicate tetrahedral group. Assuming that each of the bonds has an ionic character of 49 percent and a bond number of 1.55, he calculated a charge of +0.96 (= 4 − 4 × 0.49 × 1.55) on Si in conformity with his electroneutrality principle (Pauling, 1948, 1952). About ten years ago, Collins, Cruickshank and Breeze (1972) completed calculations for the molecules SiO_4^{4-} and H_4SiO_4 with a minimal basis plus *d*-type AO's on Si and concluded that the *d*-orbitals may make a significant contribution to the molecular wave functions. In addition to finding a rather large number of electrons occupying these orbitals, they also observed that the $L_{2,3}$ X-ray fluorescence spectra of solid and amorphous silica could be reproduced only when the *d*-orbitals were included in the basis set. However, in spite of their success in rationalizing and reproducing the $L_{2,3}$ X-ray fluorescence spectra of silica, there has been a rather protracted discussion in the literature regarding the significance of these orbitals (Baur, 1971, 1977, 1978; Gilbert, Stevens, Schrenk, Yoshimine and Bagus, 1973; Griscom, 1977). For example, Gilbert *et al.* (1973) observed in a study of an extended basis calculation for molecular Si_2O that the five *d*-orbitals on Si make a relatively unimportant contribution to the wave functions of the linear molecule and that the large population obtained in the Collins *et al.* (1972) calculations for H_4SiO_4 may be an artifact of a poor basis set.

In an effort to clarify the extent to which these orbitals might contribute to the structure of the SiO bond in H_4SiO_4, Newton and Gibbs (1980) completed STO-3G* and "split valence" *s,p* basis 66-31G* calculations for the molecule. As both calculations yielded essentially the same 3*d*-orbital populations, they suggested that the populations are qualitatively significant and not an artifact of a poor basis as indicated by Gilbert *et al.* (1973). Optimization of the SiO bond lengths of the molecule with a STO-3G* basis, yielded an equilibrium bond length of 1.60Å, well within the range of recorded values in the silicate tetrahedra of the monosilicates. Thus, the STO-3G and STO-3G* calculations yield bond lengths that bracket the observed SiO bond lengths in these minerals, notwithstanding the neglect of a Madelung potential in the calculations. Also, despite the lack of constraints in the calculations, the ratio of the charges on Si and O was found to be almost exactly 2 to 1, the expected ratio for a silicate. As predicted by Pauling, the charge on Si is reduced from +1.36 to +0.81 when the minimal basis set for the molecule is augmented with the manifold of five *d*-orbitals on Si.

Deformation density maps for four-coordinate Si

Hill *et al.* (1981) have calculated a deformation density map through the OSiO group in H_4SiO_4 to assess the net transfer of charge from Si and O into the SiO bond for four coordinate Si. Calculated using a 66-31G* basis with *d*-type polarization functions, the theoretical deformation density was obtained by subtracting the superimposed densities of the component atoms of the molecule (*i.e.*, the

promolecule), from the molecular charge density, each atom being located at its appropriate position. The resulting map, displayed in Figure 3a, shows a modest accumulation of electron density in the SiO bond with the peak appreciably shifted from the midpoint of the bond in the direction of the oxygen atom as expected from electronegativity considerations. The peak has a height of 0.32 $eÅ^{-3}$ and is situated 0.65Å from the oxygen in close agreement with the Bragg–Slater atomic radius of the atom (Slater, 1972). In contrast, the minimum in the total electron density distribution along the bond (Bader, Keeveny and Cade, 1967) indicates an oxide ion radius of 0.95Å compared with the somewhat larger "ionic radius" of the ion in MgO and CaO (1.12 and 1.19Å, respectively) determined by Bukowinski (1980, 1981) and a crystal radius of 1.22Å reported by Shannon and Prewitt (1969). On the other hand, Johnson (1973) has proposed a variable oxide ion radius which decreases linearly from 1.4 to 0.8Å as the field strength of the cation bonded to it increases from K^+ to Be^{2+}. Clearly this topic warrants further study.

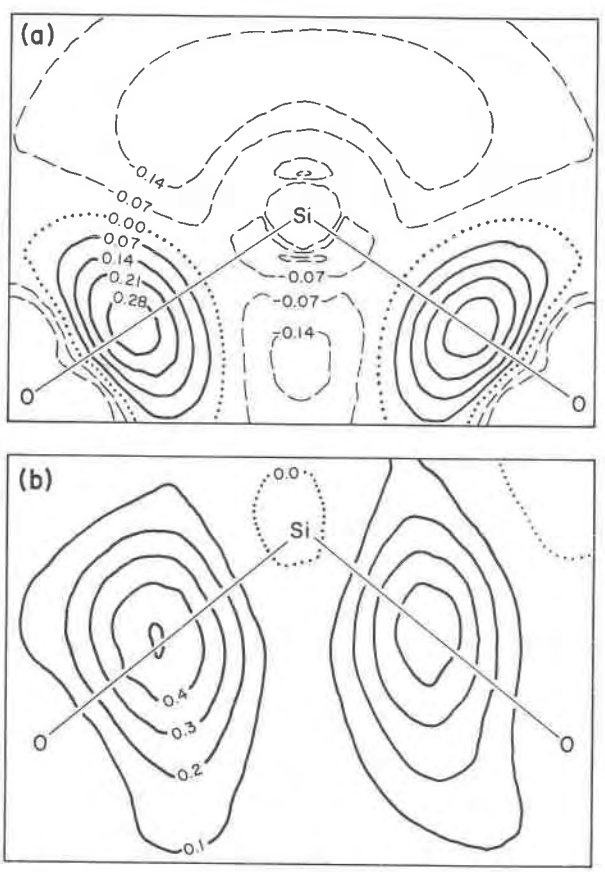

Fig. 3. A comparison of a theoretical difference deformation map (after Hill *et al.*, 1981) (a) of the OSiO group in the monosilicic acid molecule with an experimental map (b) of the group in the monosilicate andalusite, Al_2SiO_5. The contour interval is drawn at 0.07 electrons A^{-3} in (a) and 0.10 e A^{-3} in (b). The region about the nucleus of each atom in the theoretical map represents the core region where the theoretical deformation map is not expected to be accurate.

Despite the large number of structural analyses completed for the monosilicates, only a few have been undertaken to record the deformation density of the tetrahedral silicate group with which a map of the theoretical density may be compared. A survey of these studies reveals a fluctuation in the SiO bonding peak heights ranging from 0.15 to 0.80 $eÅ^{-3}$ with an average height of 0.35 $eÅ^{-3}$. In addition, the distances between the oxygen atoms and the bonding peaks range between 0.60 and 1.05Å with an average separation of 0.75Å. The main features in the experimental maps conform, on the average, with those displayed in the theoretical map. For sake of comparison, the experimental map for the silicate group in the monosilicate andalusite (Peterson, 1980) is displayed in Figure 3b with the theoretical one calculated for the monosilicic acid molecule. Despite the dissimilar bonding environments, the two maps show a resemblance which lends credence to the applicability and transferability of the molecular wave functions and property functions to analogous solid materials. In addition, both theory and experiment indicate a charge density distribution like that expected from a bond manifesting significant covalent character. As the theoretical map was obtained from static wavefunctions calculated at absolute zero without zero point motion, the comparison in Figure 3 is perforce qualitative. For the comparison to be quantitative, the theoretical density must be averaged over the appropriate vibrational states of the molecule. Nonetheless, since the Debye temperature of a monosilicate is large and since the zero point motion is not expected to have a gross effect on the distribution, the thermally smeared distribution of a theoretical map should not depart significantly from that of the unsmeared distribution displayed in Figure 3a (Spackman, Stewart and LePage, 1981).

Octahedral silicate group

By far the vast majority of silicates contain four-coordinate silicon. Nonetheless, Si is six-coordinate in such high pressure silicates as SiO_2 (stishovite) with the rutile structure, $MgSiO_3$ with the

ilmenite and perovskite structures and $KAlSi_3O_8$ with the hollandite structure and in such low pressure silicates as SiP_2O_7 and thaumasite, $Ca_3Si(OH)_6SO_4CO_312H_2O$. Also, in the moderately high pressure phase $K_2Si^{VI}Si_3^{IV}O_9$ (Swanson and Prewitt, in prep.), Si occurs in both four-coordination in 3-membered rings and in six-coordination in octahedra, linking the rings together into a three-dimensional structure. Earlier, with the first synthesis of stishovite, it was assumed that six-coordinate Si was adopted only in phases formed at high pressures. But, with the discovery of six-coordinate Si in the molecular crystals tris(O-phenylenedioxy) siliconate (Flynn and Boer, 1969), tris(acetylacetonato)silicon(IV)perchlorate and tristhylammoniumtris (pyrocatochloro)silicate (Adams, Debaerdemacker and Thewalt, 1979), it is now recognized that high pressure is not essential for the synthesis of phases with octahedrally coordinate Si. In fact, an examination of the low pressure phases shows (unlike the high pressure phases) that the oxygen atoms bonded to Si are also bonded to atoms like H, C and P whose electronegativities are greater than that of Si. According to Edge and Taylor (1971) and Liebau (1971), these atoms drain electrons from the SiO bonds, thus weakening and lengthening them and reducing their mutual repulsions to the extent that four-coordinate Si tends to be destabilized relative to six-coordinate Si. Under these conditions, the oxygen atoms are believed to behave like the fluoride atoms in the SiF_6^{2-} ion which is readily formed in phases produced at low pressures. On the other hand, Shannon, Chenavas and Joubert (1975) have pointed out that six-coordinate Si in thaumasite and SiP_2O_7 can be explained equally well in terms of the sum of bond strengths, p_o, reaching the oxygen atoms bonded to Si. For example, as p_o increases, particularly in excess of 2.0, the SiO bonds in a tetrahedral group will tend to weaken and lengthen until a critical value is reached and six-coordinate Si is adopted, thereby reducing the bond strength sum to a value in better agreement with the saturated value of 2.0.

In his pioneering work on the chemistry of silica, Iler (1955, 1979) made the proposal that the hexoxosilicate ion, $Si(OH)_6^{2-}$, forms in aqueous environments as an intermediate product in the polymerization of silicic acid. Since data are lacking for this proposal, Gibbs *et al.* (1981) undertook an analysis of the anion to explore whether there is any theoretical reason why it might not form and to see how well the anion might model the SiO bond lengths of the hexoxosilicate ion in the mineral thaumansite (Edge and Taylor, 1971). For the calculation, the anion was assumed to consist of a Si atom bonded to six hydroxyl groups each disposed at the corners of an octahedron with the SiOH angles set at 109.47° and with hydrogen fixed at 0.96Å from each oxygen atom (Fig. 4a). The minimum energy SiO bond length of the anion was obtained from a potential energy curve calculated with a STO-3G basis set. As the calculations converged rapidly and yielded a minimum energy bond length of 1.77Å in close agreement with the average bond length (1.78Å) of the anion in thaumasite, there is no apparent reason why the anion might not form as an intermediate in an aqueous environment containing the monosilicic acid molecule. But, on the other hand, Raman and ^{29}Si NMR studies of the constitution of various aqueous sodium silicate solutions indicate that the predominant form of the silicate group is probably tetrahedral (Earley, Fortnum, Wojcicki and Edwards, 1959; Freund, 1973; Englehardt, Zeigan, Jancke, Hoebbel and Wieker, 1975).

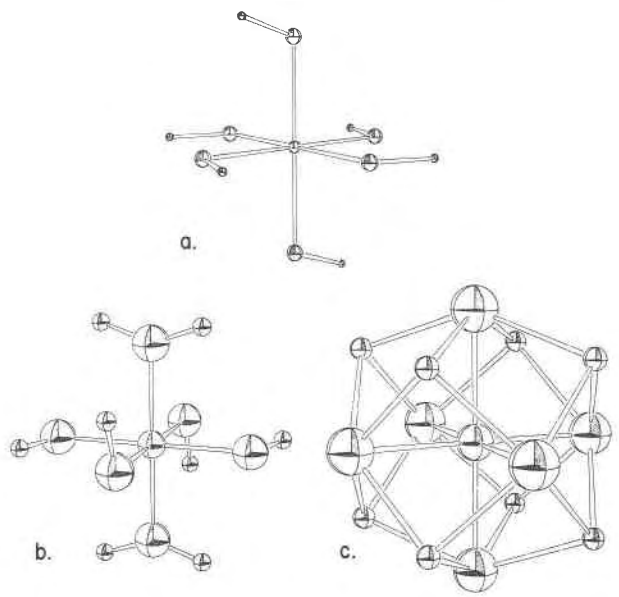

Fig. 4. Drawings of the molecules (a) $Si(OH)_6^{2-}$, (b) $Si(OH)_4(OH_2)_2$ and (c) H_8SiO_6. The silicon atom centering each of these molecules is represented by an intermediate-size sphere, the six coordinating oxygen atoms disposed at the corners of a perfect octahedron are each represented by a large sphere, and the hydrogen atoms attached to the oxygen atoms are each represented by a small sphere. The point symmetries of $Si(OH)_6$ and $Si(OH)_4(OH_2)_2$ are both C_i whereas that of H_8SiO_6 is H_h. No significance is attached to the relative sizes of the spheres used to represent the atoms. (After Hill *et al.*, 1981.)

Since the hexoxosilicate ion discussed above is negatively charged, its minimum energy SiO bond length may not be comparable with that of a solid like stishovite.[3] Thus, in their study of the crystal chemistry of stishovite, Hill *et al.* (1981) optimized the SiO bond lengths of the neutral $Si(OH)_4(OH_2)_2$ molecule. They formed this molecule by adding two protons to $Si(OH)_6^{2-}$, converting two hydroxyl groups on opposite ends of the molecule to water molecules (Fig. 4b). Optimization of the SiO bond length, R(SiO), assuming that all the bonds are equivalent, yielded a slightly shorter minimum energy value of 1.75Å compared with the average bond length (1.77Å) observed for a number of silicates and silicate molecular crystals with six-coordinate Si (Fig. 5). The quadratic stretching force constant calculated from the curvature of the potential energy curve is 540 Nm^{-1}, about 10 percent less than that calculated for four-coordinate Si in monosilicic acid. The larger force constant of the bond in the latter molecule is consistent with its shorter bond length and smaller coordination number.

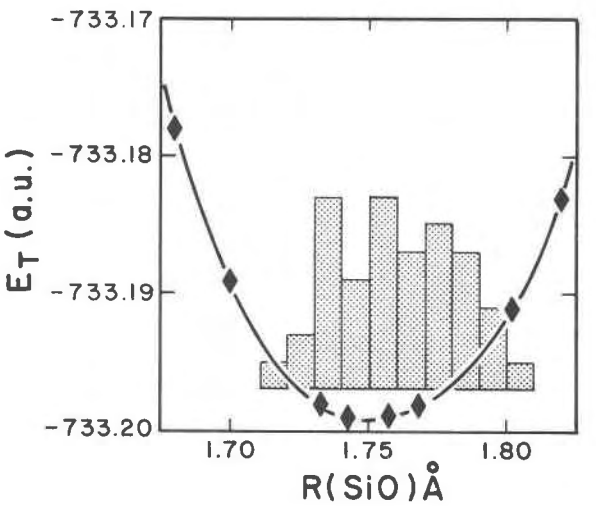

Fig. 5. A potential energy curve calculated for $Si(OH)_4(OH_2)_2$ (see Fig. 4b) as a function of the SiO bond length, R(SiO). In the calculation of the total energy, E_T, all R(SiO) values were considered as equivalent. A frequency distribution of experimental SiO bond lengths in silicates and siloxane molecular crystals with six-coordinate silicon is superimposed on the drawing. The average bond length for the distribution is 1.77Å compared with a minimum energy bond length of 1.75Å. (Modified after Hill *et al.*, 1981.)

Si3d orbital population

In a study of six-coordinate second row cations, Tossell (1975) undertook an X_α Scattered Wave calculation for the highly charged holosilicate ion, SiO_6^{8-}, when investigating variations in the electronic structure of the oxyanions MgO_6^{10-}, AlO_6^{9-} and SiO_6^{8-}. As expected from electronegativity considerations, the calculations indicate a substantial increase in covalency in the series as evinced by an increase in the width of the valence band. However, the paucity of experimental data prevented comparing these calculated spectral data to those of stishovite. In addition, as Tossell's X_α results for the ion indicate that the higher energy $1t_{2g}$-type Si3*d* AO's are associated with a smaller fraction of electron density in the interatomic region than the $2e_g$-type AO's, he concluded that evidence is lacking for the d^2sp^3 hybridization model proposed for hexacoordinate Si compounds by Voronkov, Yuzhelevskii and Mileshkevich (1975). In a later CNDO/2 MO study of the X-ray emission and absorption spectra of stishovite, Brytov, Romashchenko and Shchegolev (1979) reported 0.9 electrons in the $1t_{2g}$-type AO's and 1.0 in the $2e_g$-type AO's of the holosilicate ion. An examination of the STO-3G* wave functions described above for the $Si(OH)_4(OH_2)_2$ molecule indicates a somewhat smaller population of 3*d* electrons, with 0.6 electrons in the $2e_g$-type and 0.3 in the $1t_{2g}$-type AO's. A 66-31G* basis calculation for the molecule indicates 0.4 electrons in the $2e_g$-type and 0.2 in the $1t_{2g}$-type AO's, for a total of 0.6 electrons in the 3*d* AO's of Si (Hill *et al.*, 1981). Also, a total of 0.6 electrons was obtained in these AO's in similar calculations for SiO_2 and H_4SiO_4 molecules (Pacansky and Hermann, 1978; Newton and Gibbs, 1980). Thus, the 3*d* type polarization functions on Si seem to make about the same contribution to the wave function of a molecule regardless of the coordination number of Si.

A population analysis of the STO-3G wave functions of $Si(OH)_4(OH_2)_2$ yielded a charge of +1.40 on Si compared with +1.36 obtained for four-coordinate Si in H_4SiO_4. However, the charge on the six-

[3]In a bond length study of solids and chemically similar molecules, Gibbs *et al.* (1981) found that the calculated bond lengths for neutral molecules agree to within 0.02Å, on the average, with those in chemically similar solids. On the other hand, those calculated for highly charged molecules were found to depart from experimental values, on the average, by 0.07Å in length. Gupta and Tossell (1981) ascribe this poor agreement to electron–electron repulsions between the extra electrons. As electrostatic neutrality generally obtains within the fundamental domain of a solid, the values for highly charged molecules are not expected to be comparable with those in chemically related solids.

coordinate Si is reduced to +0.74 when the 3*d* type AO's of Si are added to the basis set. This charge compares favorably with that (+0.97 = 4 − 6 × 1.03 × 0.49) calculated with Pauling's (1952) method for a six-coordinate SiO bond length of 1.76Å. It is noteworthy that Pauling's method yields a charge of ~ +1.0 on Si regardless of whether it is bonded to either four or six oxygen atoms. Nonetheless, as the charge on an atom in a molecule or a solid is arbitrary and not an observable, there is no experimental technique that can be used to verify these numbers (Stewart and Spackman, 1981).

Deformation density maps for six-coordinate Si

Of the silicates with six-coordinate Si, stishovite is the only one for which deformation density maps have been produced from X-ray diffraction data. Actually, because of its chemical and structural simplicity, the mineral is ideally suited for such a charge density study. The structure of the mineral consists of a framework of corner and edge sharing silicate octahedral groups. As the octahedral sharing coefficient is 3.0, each oxygen atom in the mineral is bonded to three Si atoms lying at the corners of a triangle. The Si atoms occupy octahedra that share opposite edges with other octahedra to form interconnected octahedral chains along *c*.

A deformation map calculated through a SiO_4 plane of one of these octahedra is displayed in Figure 6a (Hill *et al.*, 1981). The most prominent features in the map are peaks of electron density in each bond located about 0.68Å on the average from oxygen. As may be expected, the peaks in the shorter equatorial bond are significantly larger (0.47e $Å^{-3}$) than those in the longer apical bonds (0.29 $eÅ^{-3}$). Interestingly, these peaks have about the same heights as those recorded for the SiO bonds in the monosilicates. On the other hand, the bonding peaks in stishovite are significantly smaller than those (~0.85 eA^{-3}) in α-quartz, where the bonds are ~0.2Å shorter in length. However, we are unable to offer a satisfactory explanation of why the peak heights in the monosilicates are significantly smaller on the average than those in α-quartz.

To assess the net charge transfer of electrons from Si and O into the SiO bond for six-coordinate Si, Hill *et al.* (1981) completed "split valence" 66-31G* calculations for two different molecules with six coordinate Si. In devising the topology of these molecules, they considered three factors: (1) the simulation of the bonding requirements of both Si and O; (2) the flexibility of an adequate AO basis set; and (3) computational feasibility. Earlier studies by Newton and Gibbs (1979) on the disiloxane molecule indicate that a 66-31G* basis is required to yield qualitatively meaningful deformation densities. Because of the very large size of this basis, computational feasibility limited it to molecules with a few atoms, thus placing severe constraints on its ability to model the Si and O environment in stishovite. With these limitations in mind, Hill *et al.* (1981) completed calculations for the two following molecules: (1) the $Si(OH)_4(OH_2)_2$ molecule (Fig. 4b) and (2) an octahedral molecule with the same formula (H_8SiO_6), but with the eight H atoms symmetrically arranged on the 3-fold axes of the SiO_6 octahedral group in conformity with O_h (= $4/m\bar{3}2/m$) point symmetry (Fig. 4c).

The deformation map for the $Si(OH)_4(OH_2)_2$ molecule was deficient as a model for the six-coordinate Si in stishovite in that it lacked any significant build up of electron density in the SiO bonds of the molecule. At first glance, the H_8SiO_6 molecule may also seem to be deficient as a model, but a careful scrutiny of its topology shows that it satisfies the bond strength sum requirements in stishovite, *i.e.*, the bond strength sum to each oxygen atom is exactly 2.0. Moreover, the features of a deformation map calculated for a SiO_4 plane of the molecule are similar to those in the experimental map for stishovite (Fig. 6b). Not only are the bonding peaks in the theoretical map (0.31e $Å^{-3}$) similar in height to those in stishovite, but also the peaks are located about 0.65Å from the oxygen atom compared with a bond peak to oxygen atom separation of 0.68Å in the mineral. Clearly, both theory and experiment indicate that the bonding in stishovite has appreciable covalent character, but its smaller bonding peaks relative to those in α-quartz suggest that the covalent character of the bond may be less for six- than for four-coordinate Si.

The disiloxy (SiOSi) group

Silicates exhibit a wide variety of polymerized tetrahedral silicate groups of differing topologies ranging from the oligosilicates with oligomers of corner sharing silicate tetrahedra to the tectosilicates with continuous three dimensional extensions of corner sharing tetrahedra (Liebau, 1980). The polymerized tetrahedral groups in this latter class of silicates are held intact by the important disiloxy group in contrast with the monosilicates which contain insular silicate tetrahedral groups. In the

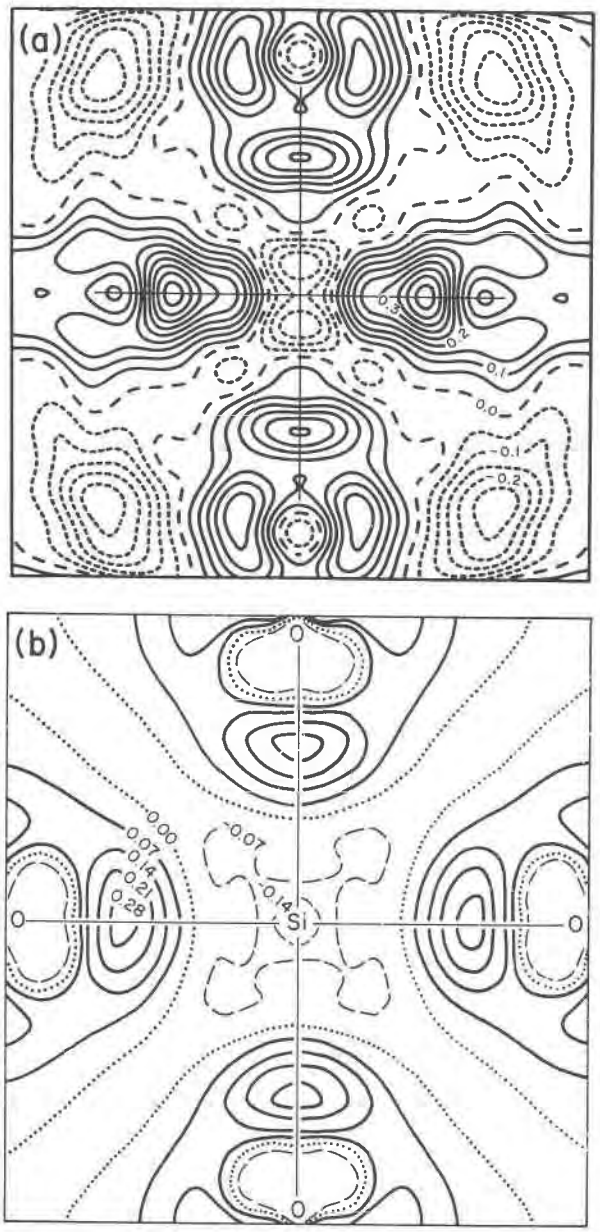

Fig. 6. An experimental deformation map (a) calculated through the apical and equatorial bonds of the holosilicate anion in stishovite, a very high pressure polymorph of SiO_2, compared with a theoretical map (b) calculated through a SiO_4 plane of the H_8SiO_6 molecule displayed in Figure 4c. The contour interval is drawn at 0.05 e A^{-3} in (a) and 0.07 e A^{-3} in (b). In (a), the zero contour is drawn as a long-dashed line, the negative contours are short-dashed lines, and the positive contours are as solid lines. (After Hill *et al.*, 1981.)

last section, we examined a series of calculations for the SiO bond in molecules with four- and six-coordinate Si and observed that the optimized bond lengths are in good agreement with those in comparable silicates. In this section, geometries and deformation density distributions generated for the molecules $H_6Si_2O_7$ and H_6Si_2O will be compared with those observed for the silica polymorphs. Then the bond lengths and angles generated for rings of disiloxy groups will be compared with those in silicate and siloxane solids.

Disiloxy groups in the silica polymorphs

The disiloxy groups in the silica polymorphs exhibit a relatively wide range of SiOSi angles, varying from about 135 to 180°. As the angle widens, the bridging bonds tend to shorten by a small yet significant amount. In fact, they appear to shorten nonlinearly when plotted against the angle but linearly when plotted against either the hybridization index, λ^2 ($= -1/\cos\angle\text{SiOSi}$ defined by the superscript sp^{λ^2}), or the fraction *s*-character, $f_s = (1 + \lambda^2)^{-1}$, of the bridging oxygen of the disiloxy group (Gibbs *et al.*, 1972; McWeeny, 1979; Newton and Gibbs, (1980). For a brief but very informative discussion of f_s as provided by the concept of hybridization, the reader is referred to an excellent paper by Newton (1981) who examines the role played by the hybrid AO's of the bridging oxygen in the disiloxy group and provides a quantum mechanical underpinning of the hybrid concept in terms of *ab initio* hybrid AO's obtained with localized molecular orbital theory.

In an attempt to elucidate the nature of the disiloxy group, Tossell and Gibbs (1978), Meagher, Tossell and Gibbs (1979), DeJong and Brown (1980a, b) and Lasaga (1982) have employed semi-empirical CNDO/2 theory to calculate a series of potential energy curves for disiloxane and various molecules containing the disilicate group and have found that the minimum energy angle for a fixed set of SiO bond lengths is in good agreement with a typical angle in the silica polymorphs. It was also found that the broad range of angles recorded for these minerals can be interpreted in terms of the shape of the curve for the disiloxane molecule (Tossell and Gibbs, 1978). In a recent study of the correlation between bond length and angle, the SiO bond lengths in disilicic acid were optimized as a function of the SiOSi angle using STO-3G theory (Newton and Gibbs, 1979, 1980). The resulting correlation displayed in Figure 7 agrees to within about 0.03Å with that observed for coesite, a high pressure polymorph of silica (Gibbs, Prewitt and Baldwin, 1977a). Also, as observed for the silica polymorphs, the mean SiO bond lengths for the

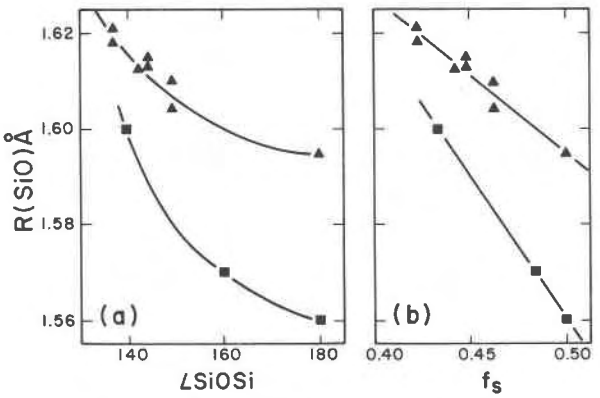

Fig. 7. A comparison of the experimental SiO bond lengths, R(SiO), in coesite, a high pressure polymorph of SiO_2, (uppermost curves in (a) and (b)) with those calculated for the bridging bonds in the disilicate molecule, $H_6Si_2O_7$, with its bridging angle being fixed in succession at 140, 160 and 180° (lowermost curves in (a) and (b)). The bond lengths in both coesite and the molecule vary nonlinearly when plotted against ∠SiOSi and linearly when plotted against $f_s = 1/(1 + \lambda^2)$ where $\lambda^2 = -1/\cos\angle SiOSi$ is called the hybridization index of the bridging oxygen atom because its state of hybridization is given by the symbol sp^{λ^2}. (After Newton and Gibbs, 1980.)

molecules decrease linearly with the hybridization index of the bridging oxygen (Meagher and Gibbs, 1976).

The energetics of the disiloxy group

In a study of the quadratic bending and stretching force constants of the disiloxy group, Newton and Gibbs (1980) used STO-3G basis functions to calculate three potential energy curves for the disilicic acid molecule, $H_6Si_2O_7$, as a function of the SiOSi angle. To maintain the average SiO bond length of the molecule at 1.62Å, the bridging bond lengths were set in succession at 1.59, 1.62, and 1.65Å, whereas the nonbridging bonds were set at 1.63, 1.62 and 1.61Å, respectively. For simplicity, the OSiO and SiOH angles were each set at 109.47° and the neutralizing protons were placed at 0.96Å from each of the nonbridging oxygen atoms. The three curves that resulted from the calculations have respective minima becoming progressively broader with each curve rising gradually with increasing angle to 180°. In contrast, the curves rise steeply (in the region of ~120°) with decreasing angle from the minima. When a three point parabola was fit to each of these curves, Newton *et al.* (1980) found that the resulting symmetric SiOSi bending constant is in rough agreement with that reported for α-quartz. They interpreted this to mean that the bonding forces in the two systems are comparable and that the force field for the group in the molecule may be applicable and transferable to α-quartz. Moreover, since the SiO stretching (~850 Nm^{-1}) and the OSiO bending (~100 Nm^{-1}) force constants are significantly larger than that of the SiOSi bending force constant (~10 Nm), the bulk modulus of the mineral was concluded to be controlled in large part by the compliant nature of the SiOSi angle. When it was assumed that the dominant contribution to the isothermal bulk modulus, K ($=V\partial P/\partial V|_T$), is the bending force constant of the SiOSi angle, the calculated bulk modulus (0.397 megabars) was found to be in good agreement with the experimental value (0.393 megabars) extrapolated to 0°K. The bending force constant, when examined as a function of the shape of the disiloxy group, was found to increase as the bond lengthened and the angle narrowed. Since the bulk modulus appears to be controlled by the compliance of the SiOSi angle, the isothermal pressure derivative of the bulk modulus should also decrease as the mineral is compressed and narrower equilibrium angles are adopted (Ross and Meagher, 1981). The isothermal pressure derivative of the bulk modulus, K′ ($= \partial K/\partial P|_T$), should also be relatively large inasmuch as the SiOSi angle should narrow at a relatively rapid rate upon initial application of pressure (Bass, Liebermann, Weidner and Finch, 1980). Eventually, when the angle is compressed to about 120°, nonbonded Si · · · Si and O · · · O, repulsions should dominate and the value K′ should approach a constant value. Finally, temperature and pressure changes should have a relatively large effect on the soft SiOSi angle while they should have a moderate effect on the OSiO angle and little effect on the stiff SiO bond in α-quartz (Levien, Prewitt and Weidner, 1980; Ross and Meagher, 1981; Lager, Jorgensen and Rotella, 1982).

Potential energy surface of the disiloxy group

In a recent examination of the energetics of the disiloxy group, Meagher *et al.* (1980) calculated the potential energy of $H_6Si_2O_7$ for more than 70 different pairs of bridging bond lengths and angles. The resulting total energies, plotted as a function of R(SiO) and ∠SiOSi and contoured, generate the surface displayed in Figure 8. A study of the surface shows for the most part that the potential energy of the group varies relatively slowly with angle in the vicinity of the minimum but relatively rapidly with

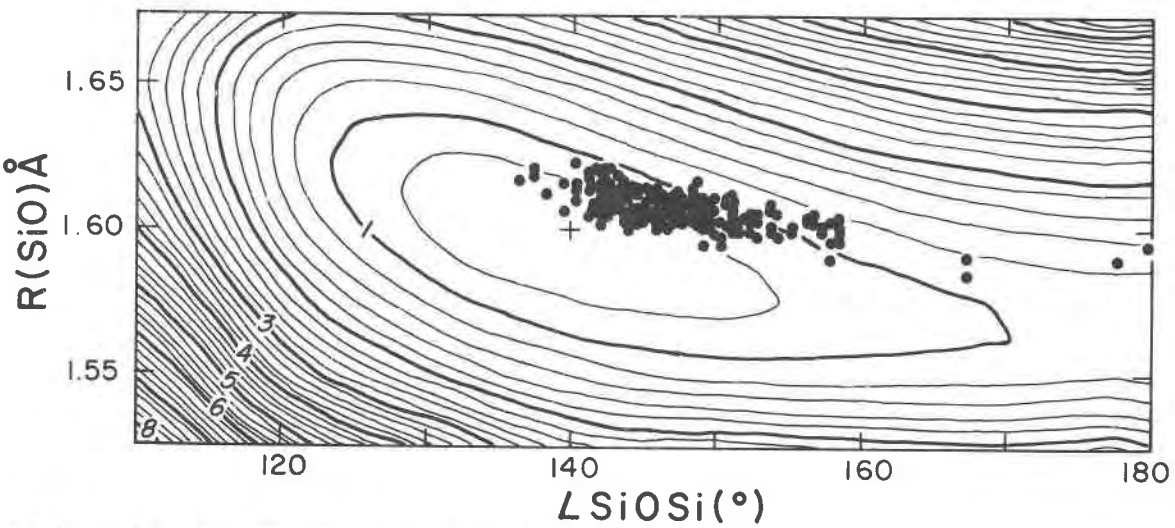

Fig. 8. A potential energy surface for the disilicate molecule, $H_6Si_2O_7$, plotted as a function of its bridging bond length, R(SiO), and SiOSi angle. The energy represented by the contours corresponds to increments of 0.001 a.u. (= 0.6257 kcal mole^{-1}) relative to the minimum energy point (−1091.76678 a.u.) denoted by a cross. For sake of convenience, the 0.005 a.u. increments are indicated by heavier lines labeled from 1 to 8 in order of increasing energy. The data points plotted on the energy surface are experimental bond lengths and angles for the disiloxy groups in the silica polymorphs coesite, tridymite, low cristobalite and α-quartz. (After Meagher *et al.*, 1980.)

change in bond length. The minimum energy configuration is located at the bottom of a relatively narrow energy valley blocked at one end and bounded laterally by steeply rising energy barriers. In contrast, the other end of the valley is bounded by a gradually rising surface. It is also observed that the valley shows a slight curvature which conforms with the curvilinear bond length–angle trend observed for coesite (Fig. 7). Superimposed upon the energy surface are the experimental bond length and angle data for the disiloxy groups in the silica polymorphs (Hill and Gibbs, 1979; Gibbs *et al.*, 1981). The data follow the general trend of the surface, but the observed bond lengths are about 0.02Å longer on the average than that defined by the valley bottom (Fig. 8). Despite this difference, which may be related to lattice vibrations at room temperature, the fact that the bond length and angle data for the silica polymorphs fall close to the valley bottom indicates that the energetics of the disiloxy group in the disilicic acid molecule may be transferred and applied as a model to account for the energetics and geometry of the group in the silica polymorphs.

The barrier to linearity is defined to be the difference between the total energy of the molecule evaluated for a straight bridging angle and that evaluated at the minimum energy angle. It is small (~ 3kT at room temperature) and indicates that a relatively small amount of energy will be expended in deforming the SiOSi angle from its minimum energy value to 180°. If the bonding forces in disilicic acid and the silica polymorphs are similar, then the SiOSi angles in the latter may be readily deformed from their equilibrium values to form a periodic extension of silicate tetrahedra without unduly destabilizing the resulting structure. Thus, a broad continuum of SiOSi angles is expected to occur in agreement with the relatively large range of observed angles. Also, because of the steep energy barrier blocking the valley at narrow angles, SiOSi angles less than ~120° are indicated to be unstable. Finally, the glass forming tendencies and the ability of silica to exist in a relatively large variety of polymorphs depending on the ambient temperature and pressure may also be ascribed in part to the flexible nature of the disiloxy group and the ease with which its angle can be deformed from its equilibrium value without excessively destabilizing the final structure.

Rings of disiloxy groups

A silicate ring of difunctional units differs from a comparable siloxane ring in that each Si atom in the siloxane ring is bonded to two bridging oxygen atoms and two nonbridging organic groups, whereas in the silicate ring each Si atom is bonded to four oxygen atoms (Noll, 1968). In spite of this impor-

tant difference, Chakoumakos *et al.* (1981) have found that a close correspondence exists in the shape of the disiloxy group in silicate and siloxane rings. The SiOSi angles in 4-, 5- and 6-membered silicate rings exhibit a wider range of angles (130 to 180°) and a wider angle on average (145°) than the 3-membered silicate rings which exhibit a range of values from 120 to 140° with an average angle of 130°. Despite a somewhat smaller range of angles (125 to 170°) and a paucity of 5- and 6-membered rings, the average angles exhibited by siloxane rings are practically the same as those observed for silicate rings (Fig. 9). Also, as observed for the silica polymorphs and other silicates (Brown *et al.*, 1969; Brown and Gibbs, 1970; Gibbs *et al.*, 1972; Gibbs *et al.*, 1974; Gibbs et al., 1977a; Hill and Gibbs, 1979), the bridging SiO bond lengths in both siloxane and silicate rings appear to shorten with increasing SiOSi angle (Ribbe, Gibbs and Hamil, 1977).

In their STO-3G calculations, Chakoumakos *et al.* (1981) optimized the SiO bond lengths and SiOSi angles for several molecules, including cyclotrisiloxane and cyclotetrasiloxane which consist of a 3- and 4-membered ring, respectively. To reduce computer costs, the calculations were made assuming R(SiH) = 1.50Å, ∠OSiH and ∠HSiH = 109.47° and various point symmetries for the molecules. As cyclotrisiloxane has yet to be isolated, no comparison could be made between its calculated and observed bond lengths and angles. On the other hand, the shape of the disiloxy group in cyclotetrasiloxane determined for a gas phase molecule (Glidewell *et al.*, 1970), shows a fairly close correspondence with that calculated (Chakoumakos *et al.*, 1981):

	obs.	calc.
R(SiO)	1.63Å	1.61Å
∠SiOSi	149°	142°
∠OSiO	112°	111°

Chakoumakos *et al.* (1981) also discovered that the

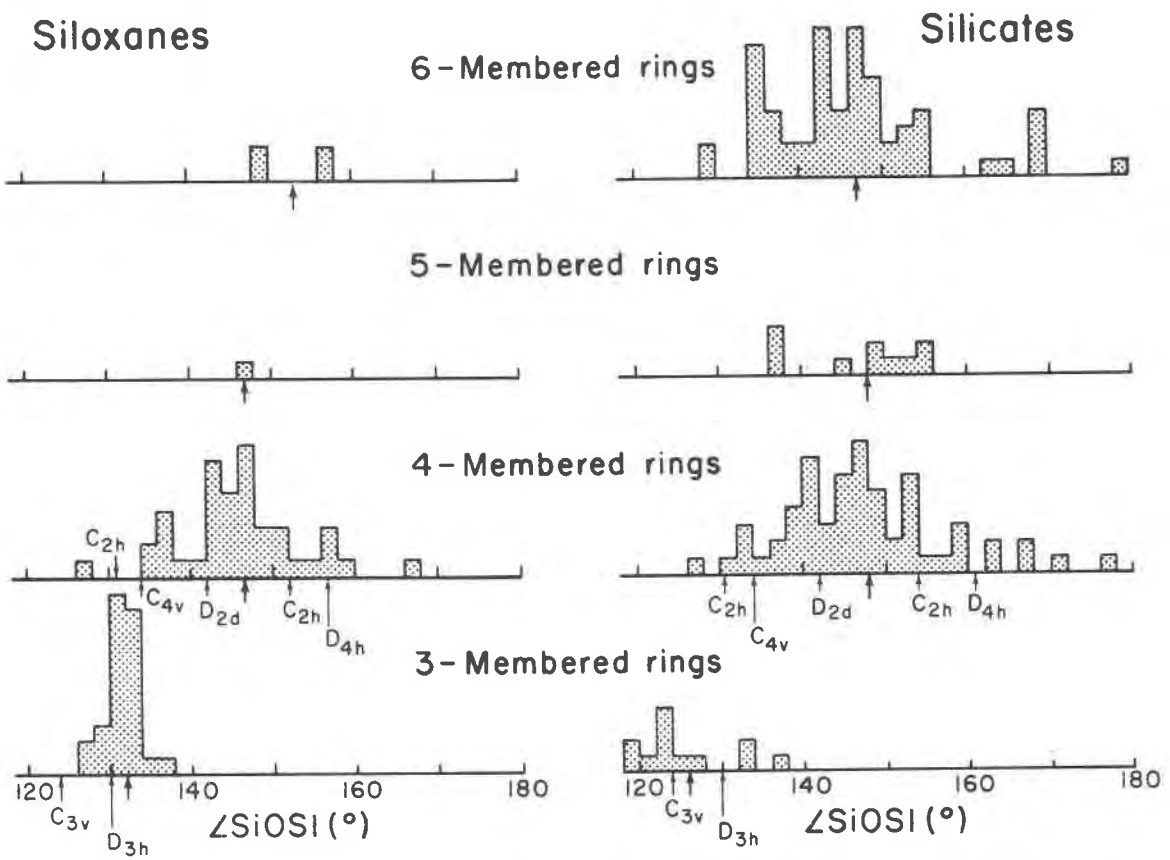

Fig. 9. The SiOSi angle frequency distributions for rings of disiloxy groups in silicates and siloxanes. The average angle for each distribution is represented by a boldface arrow while regular arrows mark the SiOSi angles of cyclotrisiloxane and cyclotetrasiloxane molecules optimized for various point symmetries. The point symmetries assumed in optimization of the angles are stated at the origin of each regular arrow. (After Chakoumakos, 1981.)

bridging bond lengths and angles calculated for these molecules reproduce the correlations displayed in Figure 10 between R(SiO) and f_s for siloxanes and silicates. Note that the calculated SiOSi angle frequency distributions plotted in Figure 9 correspond fairly well with those observed. It was also observed that the maximum SiOSi angle that a 3-membered ring of regular tetrahedra can adopt is 130°. Inasmuch as this is about 15° narrower than the minimum energy angle of the SiOSi group, they went on to suggest that the bond in a 3-membered ring is strained and less stable than that in a larger ring which may adopt a wider, more stable angle by embracing a nonplanar configuration. However, they did note that a 3-membered ring may be favored in a high pressure environment where narrower SiOSi angles are indicated to be stabilized (Ross and Meagher, 1981). Chakoumakos *et al.* (1981) also suggested that 3-membered rings should be relatively uncommon in silica glass and melts where more flexible 4-, 5- and 6-membered rings should predominate.

Deformation maps for the disiloxy group

In an earlier section of this report, we examined the tetrahedral distribution of charge density in the monosilicic acid molecule and noted a net transfer of density from Si and O into the SiO bond region in forming a polar covalent bond. In this section, a deformation map of the disiloxy group in disiloxane will be compared with a static deformation map of the group in α-quartz (Fig. 11).

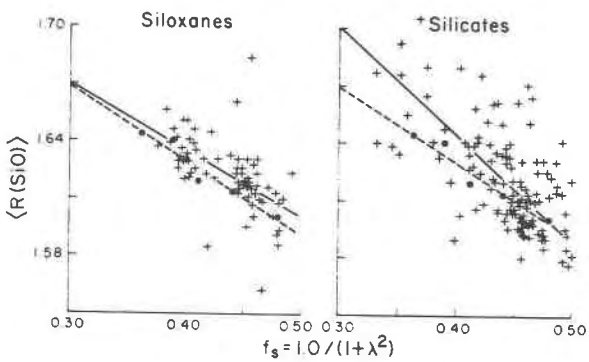

Fig. 10. Experimental SiO bond lengths, R(SiO), for rings of disiloxy groups in siloxanes (a) and silicates (b) plotted against $f_s = 1/(1 + \lambda^2)$ where $\lambda^2 = -1/\cos\angle SiOSi$. The solid lines superimposed on both figures were determined by linear regression analyses. The five data points plotted as solid circles represent theoretical values obtained by optimizing the bridging bond lengths and angles of several cyclotrisiloxane and cyclotetrasiloxane molecules with various point symmetries. The dashed lines denote regression lines fit to the theoretical data. The SiO bonds used to prepare (a) each have a bond strength sum, p_o, of exactly 2.0, whereas those used to prepare (b) have p_o values that depart from 2.0 in certain cases by as much as 35 percent. As the variation in R(SiO) is dependent upon p_o, the larger scatter of points about the regression line in (b) as compared with (a) is expected. (After Chakoumakos, 1981.)

The map of the SiOSi group in disiloxane was calculated for the observed geometry of the molecule, using a 66-31G* "split valence" basis wave function (Newton and Gibbs, in prep.). The resulting map displayed in Figure 11b indicates that there has been a transfer of electron density from the Si and O atoms to a peak in each bond and also to the lone pair region on the back side of the bridging oxygen atom. Interestingly, these peaks are offset from the line between Si and O toward the interior side of the SiOSi angle in conformity with the narrower angle between the hybrid orbitals on the bridging oxygen atom and with the suggestion (Newton, 1981) that these orbitals play a crucial role in modeling the electron density distribution of the disiloxy group. Also, in their study of disiloxane, Newton and Gibbs (in prep.) optimized the molecule's geometry using a "split valence" basis and obtained an equilibrium SiOSi angle of 149°, a SiO bond length of 1.642Å and a dipole moment of 0.32 D compared with experimental values of 144°[4], 1.634Å (Table 1), and 0.24 D (Varma, MacDiarmid and Miller, 1964).

In a mapping of the electrostatic properties from X-ray data for α-quartz, Spackman *et al.* (1981) computed a static deformation map for the disiloxy group in the mineral. This map displayed in Figure 11a represents the deformation density of the bond at absolute zero and, as such, may be compared directly with the theoretical map of the bond displayed in Figure 11b. As observed in the theoretical map for disiloxane, the bonding peaks are arcuate in shape and are situated closer to the more electronegative oxygen atom. However, the electron density goes to zero on both sides of each bonding maxima in the theoretical map in contrast with the map for α-quartz which shows the bonding peaks superimposed on a continuum of charge density between the bonded centers. In fact, the charge density distribution in α-quartz appears to be smeared more than one would expect for a localized bonding model. Also, the heights of the bonding

[4] Durig *et al.* (1977) report a SiOSi angle for disiloxane of 149±2°.

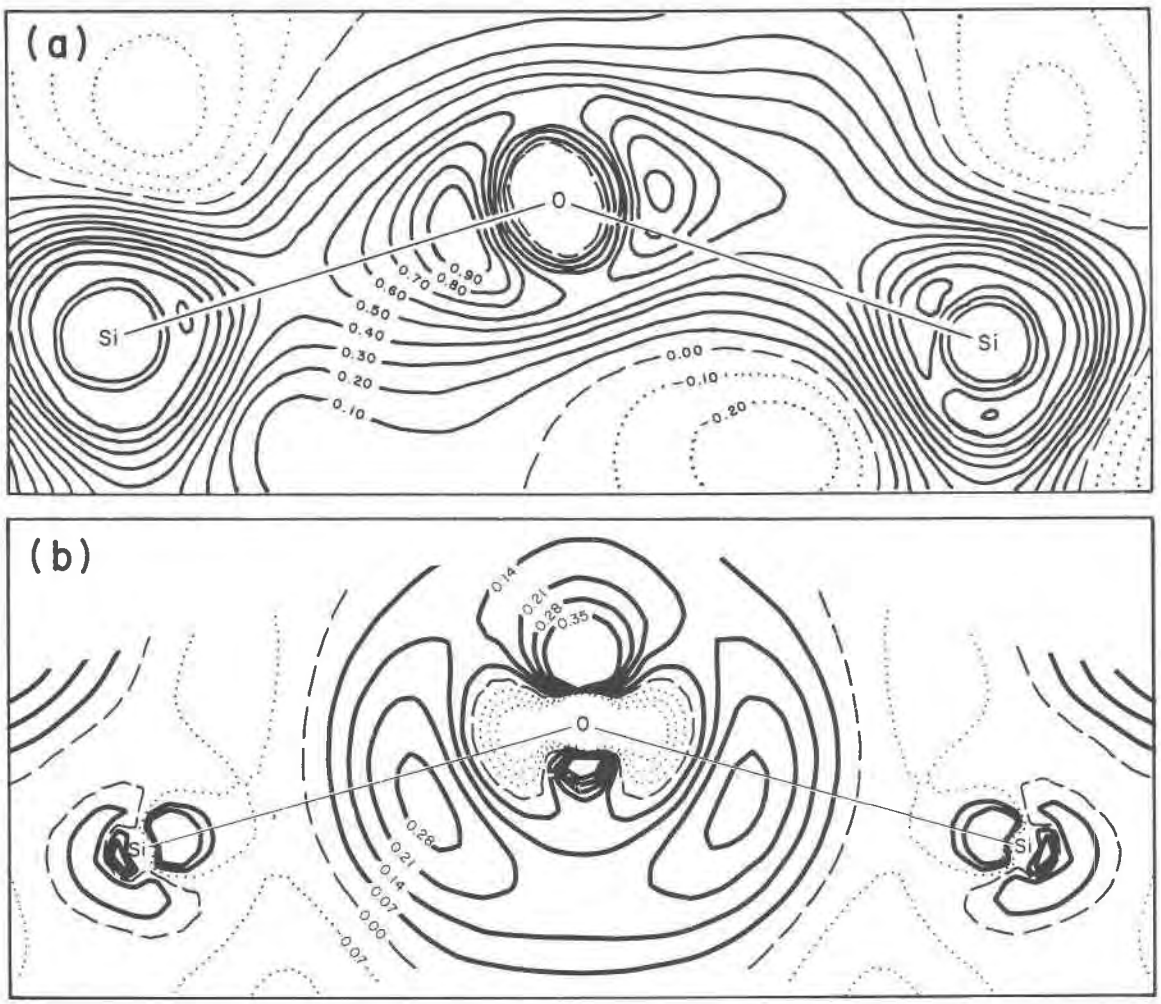

Fig. 11. Comparison of an experimental static deformation map (a) of the disiloxy group in α-quartz with a theoretical map (after Spackman et al., (1981) (b) of the bond in disiloxane calculated with a 66-31G* basis (after Gibbs and Newton, in prep.). The contours are drawn at intervals of 0.10 e A^{-3} in (a) and 0.07 e A^{-3} in (b).

peaks in the mineral are significantly larger (0.85 eA^{-3}) than those calculated for disiloxane. These peaks are even larger than those (0.6e A^{-3}) in a deformation map of the silicon monoxide molecule which was calculated at the Hartree–Fock limit (Stewart, in prep.). Nonetheless, the bonding peaks in SiO are arcuate in shape as in α-quartz and are situated closer (0.60Å) to the oxygen atom. As recorded for the disiloxane molecule, the electron density associated with the bonding peak in SiO also drops to zero between Si and O. There is, however, a conspicuous absence of charge density in α-quartz on the back side of the oxygen atoms that may be ascribed to lone pair density. To our knowledge, such an accumulation in the lone pair region has yet to be observed in a silicate.

In addition to the static maps for α-quartz, deformation maps have also been reported for the SiOSi groups in pectolite (Takeuchi and Kudoh, 1977), coesite (Gibbs *et al.*, 1978) and enstatite (Ghose, Wang, Ralph and McMullan, 1980). The charge density distributions recorded for the bonds in these minerals are in closer agreement with the theoretical map in that the bonding peaks between Si and O average 0.35e$Å^{-3}$. The electron density between Si and O drops to zero in each of these minerals rather than showing peaks superimposed on a continuum of charge density between the bonded centers as in α-quartz. The modest peaks of charge density in the bond region give the same picture of a covalent bond as was inferred from aspects of the bond such as overlap population (Gibbs *et al.*, 1972; Newton

and Gibbs, 1980). However, the bond picture is somewhat obscured in that the theoretical maps exhibit nodes between the bonding peaks and Si. This feature is observed in all the theoretical maps calculated and will be discussed at a later time (Newton and Gibbs, in prep.).

SiOT groups (T = Si, Al, B, Be)

The shape and variability of the SiOT groups in silicates

Assuming that the chemical interactions in gas-phase molecules and solids are essentially the same and that carefully selected molecules can serve as models for describing the SiOT bridging angles in solids, Tossell and Gibbs (1978), Meagher *et al.* (1979) DeJong and Brown (1980a, b) and Lasaga (1982) computed bridging angle potential energy curves for several siloxane and silicic acid molecules, using the CNDO/2 method. Not only were the average bridging angles in various silicates reproduced, but also their ranges seem to conform with the shapes of the curves. In the last section, we examined the nature of the disiloxy groups in disilicic acid and various ring silicates and showed that their equilibrium geometries conform with the bond length and angle variations in comparable silicates (within the experimental error). Then we found that the group comprises significant accumulations of bonding density in conformity with its covalent character. In this section, we will examine a similar set of curves generated for the SiOT groups in the molecules whose optimized bridging bond lengths and angles are given in Table 2. As observed in the Tossell and Gibbs (1978) study, the range of angles in solids conforms for the most part with the energetics of the bridging bonds in various silicate molecules (Downs and Gibbs, 1981; Geisinger and Gibbs, 1981b). Equally important, we will show that the bond length and angle trends provided by these molecules mimic experimental trends between R(TO), f_s and the bond strength sum to the oxygen atom.

The tetrahedral bond lengths and angles of the molecules listed in Table 2 were optimized with their OTO and TOH angles fixed at 109.47° and their OH bond lengths fixed at 0.96Å (Fig. 12a). The hydrogen atoms bonded to the bridging oxygens of the $H_6T_2O_6(OH)$ molecules in Table 2b were located in the plane of the bridging angle, bisecting its exterior angle (Fig. 12b). An examination of Table 2 shows, despite the relatively large variation of the individual SiO bond lengths (~0.10Å), that the mean SiO bond length for each molecule deviates, on the average, by only 0.01Å from the grand mean SiO bond length. By the same token, the individual AlO, BO and BeO bond lengths show a similar variation, but again the individual mean bond

Table 2: Optimized bond lengths (Å) and angles (°) for T_1OT_2 bonds in $H_6T_1T_2O_7$ and $H_7T_1T_2O_7$ molecules (see Fig. 12); p_o is the bond strength sum to the bridging oxygen and $f_s = 1/(1 + \lambda^2)$ where $\lambda^2 = -\sec\angle T_1OT_2$

	$R(T_1O)_{br}$	$R(T_2O)_{br}$	$R(T_1O)_{nbr}$	$R(T_2O)_{nbr}$	$\angle T_1OT_2$	p_o	f_s	Ref.
(a) $H_6T_1T_2O_7$ molecules								
H_6SiSiO_7	1.60	1.60	1.66	1.66	142	2.00	0.441	a,b,c
H_6SiAlO_7	1.59	1.69	1.67	1.72	136	1.75	0.418	b,c
$H_6SiBO_7^{1-}$	1.60	1.44	1.64	1.48	126	1.75	0.364	c
$H_6SiBeO_7^{2-}$	1.58	1.60	1.68	1.62	131	1.50	0.396	d
$H_6AlAlO_7^{2-}$	1.65	1.65	1.74	1.74	150	1.50	0.469	c
$H_6BBO_7^{2-}$	1.41	1.41	1.49	1.49	133	1.50	0.405	c
(b) $H_7T_1T_2O_7$ molecules								
$H_7SiSiO_7^{1+}$	1.71	1.71	1.65	1.65	132	3.00	0.401	c
H_7SiAlO_7	1.67	1.80	1.65	1.70	133	2.75	0.401	c
H_7SiBO_7	1.67	1.51	1.65	1.45	128	2.75	0.381	c
$H_7SiBeO_7^{1-}$	1.65	1.66	1.66	1.58	129	2.50	0.386	d
$H_7AlAlO_7^{1-}$	1.76	1.76	1.71	1.71	140	2.50	0.434	c
$H_7BBO_7^{1-}$	1.49	1.49	1.46	1.46	137	2.50	0.422	c

[a] Newton and Gibbs (1980)
[b] Meagher et al. (1980)
[c] Geisinger and Gibbs (1981)
[d] Downs and Gibbs (1981)

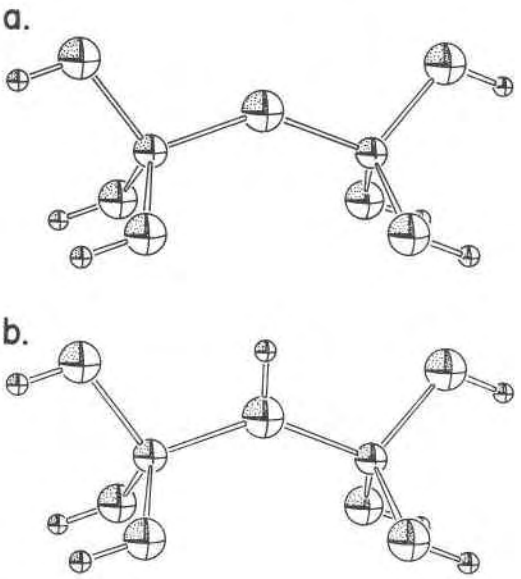

Fig. 12. Drawings of the molecular structures of H_6SiTO_7 (a) and H_7SiTO_7 (b). The intermediate-sized spheres represent the tetrahedrally coordinated Si and T (= Si, Al, B, Be) atoms, the large spheres represent oxygen and the small spheres represent hydrogen. No distinction is made in the drawings between Si and T atoms. The bridging oxygen is only bonded to a Si and a T atom in H_8SiTO_7, whereas it is bonded to Si, T and H in H_7SiTO_7. Hence, the p_o value of H_7SiTO_7 is one unit larger than that of H_6SiTO_7. No significance is attached to the relative sizes of the spheres in the molecules. (After Geisinger and Gibbs, 1981.)

lengths deviate by only 0.01Å from their grand means. Interestingly, Smith and Bailey (1963) reported a similar variation in bond distances in an important review of AlO and SiO tetrahedral bond lengths. With the equilibrium TO bond lengths given in Table 2, potential energy curves were calculated for the molecules $H_6Si_2O_7$, $H_6SiAlO_7^{1-}$, $H_6SiBO_7^{1-}$ and $H_6SiBeO_7^{2-}$ as a function of the bridging angles between 110 and 180°. The resultant curves (Fig. 13) are similar in that each shows a minimum in the region between 125 and 145° and each rises steeply with decreasing angle in the vicinity of 110–120°. This agrees with hybridization arguments by Coulson (1973) which imply that the directions of the hybrid orbitals on the bridging oxygen, and hence the SiOT angle, must exceed 90°. Clearly, the calculated angles having minimum energy decrease in the series SiOSi, SiOAl, SiOBe and SiOB with a concomitant increase in the barrier to linearity. It is noteworthy that the barrier to linearity seems in general to vary directly with the equilibrium angle, the narrower the angle, the larger the barrier. In addition, Geisinger and Gibbs (1981b) and Downs and Gibbs (1981) have found that the minimum energy SiO, AlO, BO and BeO bond lengths (Table 2) agree within the expected error with experimental values obtained for a number of silicates (Fig. 14). When the frequency distributions of the SiOSi, SiOAl, SiOBe and SiOB angles in solid silicates were superimposed on the graphs in Figure 13, they found that the average angle obtained for each population agrees to within a few degrees of the minimum energy angle obtained in the calculations:

Group	Minimum energy angle(°)	Average SiOT angle(°)
SiOSi	142	145
SiOAl	136	138
SiOBe	131	127
SiOB	126	129

Unlike the potential energy-angle curves generated for $H_6Si_2O_7$ and $H_6SiAlO_7^{1-}$, both curves for $H_6SiBO_7^{1-}$ and $H_6SiBeO_7^{2-}$ show relatively larger barriers to linearity, indicating that the range of SiOB and SiOBe angles in solids and molecules should be somewhat less than that observed for materials with SiOSi and SiOAl angles. An examination of the frequency distributions in Figure 13 shows that their angles conform with the energetics of the curves, *i.e.*, ∠SiOB and ∠SiOBe range from 120 to 142° and 118 to 152°, respectively, while ∠SiOSi and ∠SiOAl range from 120 to 180° and 115 to 180°, respectively. Thus, not only are molecular orbital generated potential energy curves capable of reproducing the shapes of SiOT groups in silicates, but they also provide important insight into the variability of their angles in solid silicates containing other tetrahedral atoms.

When a proton is attached to the bridging oxygen of an $H_6T_2O_7$ molecule, the barrier to linearity increases significantly, suggesting that the variability of a given angle should be reduced with increased coordination number of the bridging oxygen (Geisinger and Gibbs, 1981b; Downs and Gibbs, 1981). A study of the SiOSi groups for the disilicates tabulated by Baur (1971) shows that the SiOSi angle for two-coordinate oxygen ranges between 130 and 180° whereas the angle for three-coordinate oxygen is less variable and ranges between 124 and 137°. Thus, if each bridging oxygen atom in a structure is three-coordinate, then the range of bridging angles is indicated to be relatively narrow. In contrast, when some oxygens in a structure are two-coordinate, then the range of angles is relatively large

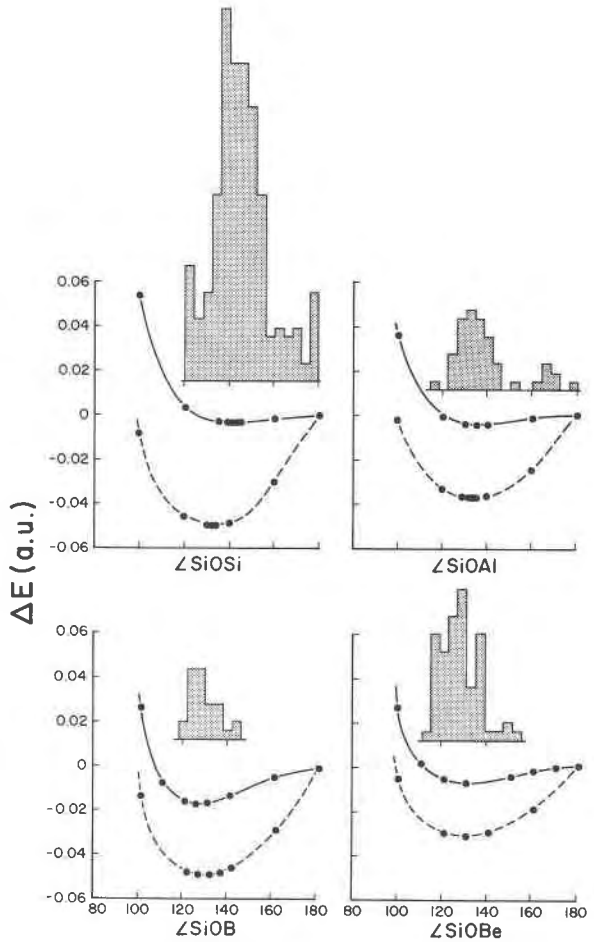

Fig. 13. Potential energy curves for the H_6SiTO_7 and H_7SiTO_7 molecules (T = Si, Al, B, Be) displayed as a function of (a) ∠SiOSi, (b) ∠SiOAl, (c) ∠SiOB and (d) ∠SiOBe (after Downs and Gibbs, 1981). Each curve was calculated using the optimized bridging bond lengths given in Table 2; the solid and dashed curves were calculated for H_6SiTO_7 and H_7SiTO_7, respectively. The histogram superimposed above each pair of curves is a frequency distribution of the experimental SiOT bridging angles recorded for various silicates. (After Geisinger and Gibbs, 1981b.)

whether or not other three-coordinate oxygens are present. In addition, the typical angle for the three-coordinate oxygen atoms in the disilicates is significantly narrower on the average (~132°) than that for the entire population (~144°). The theoretical curves for $H_6Si_2O_7$ and $H_7Si_2O_7^{1+}$ (Geisinger and Gibbs, 1981b) corroborate these results. Not only is the barrier to linearity of $H_7Si_2O_7^{1+}$ (~0.02 a.u.) with a three-coordinate bridging oxygen larger than that for $H_6Si_2O_7$, but the minimum energy angle for $H_7Si_2O_7^{1+}$ is about 10° narrower than that for $H_6Si_2O_7$ (Table 2).

The energetics of the disilathia and disiloxy groups—a comparison

The basic moiety in the thiosilicates is the tetrahedral thiosilicate group consisting of a Si atom bonded to four sulfur atoms disposed, on the average, at the corners of a tetrahedron. Even though the SiS bond is ~0.5Å longer than its SiO counterpart, the range of bond lengths (0.19Å) in thiosilicates is the same as that observed in silicates. However, in contrast with the silicates, not only do the thiosilicates show a much narrower range of bridging angles (106–115°), but they also show a more limited assortment of tetrahedral topologies. In a study of these differences, Geisinger and Gibbs (1981) found in a series of STO-3G calculations that the barrier to linearity of the disilathia group is more than a magnitude larger than that calculated for the disiloxy group. Their calculations also yielded a minimum energy SiSSi angle of 111° and bridging bond length of 2.11Å compared with averaged experimental values in molecules and solids of 110.3° and 2.13Å, respectively.

Geisinger and Gibbs (1981a) have indicated that the assortment of tetrahedral topologies exhibited by a compound should be related in part to the barrier to linearity and to the relative stiffness of the bridging angle, the greater the barrier and stiffness of the angle, the more restricted the assortment of

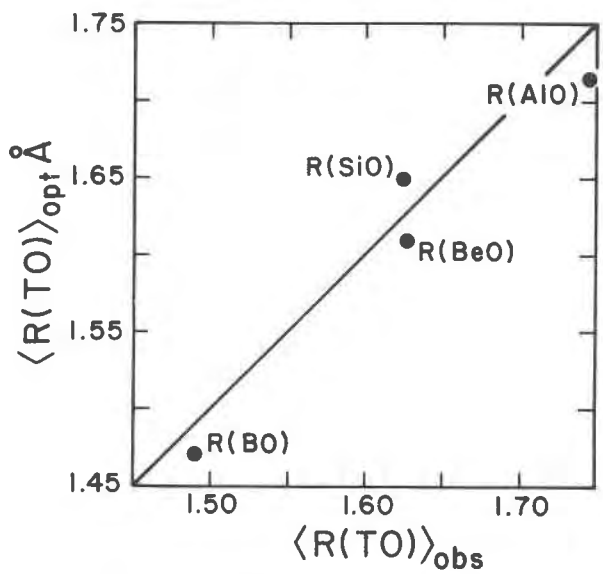

Fig. 14. The averaged tetrahedral bond lengths, $\langle R(TO)\rangle_{opt.}$, optimized for the molecules in Table 2 *versus* the averaged bridging bond lengths, $\langle R(TO)\rangle_{obs.}$, involving the angles used to prepare the histograms in Figure 13. The 45° line represents the points of perfect agreement. (After Geisinger and Gibbs, 1981b.)

stable tetrahedral topologies. As the SiOSi angle is compliant and has a small barrier to linearity, the constituent tetrahedra in a silicate may bond together in a wide range of angles, allowing a large assortment of polymeric groups of similar energies to form. On the other hand, the more limited assortment of tetrahedral topologies in the thiosilicates may be related to the larger barrier to linearity and to the greater stiffness of the SiSSi angle. Geisinger and Gibbs (1981a) also suggested that the narrow distribution of bridging angles in the thiosilicates may inhibit the formation of SiS_2 as a glass inasmuch as nearly the same SiSSi angle should be adopted and repeated again and again as in a solid.

The effect of p_o and f_s on the variation of R(TO) (T = Si, Al) in the tectosilicates

Few rules have had a more profound effect on our thinking in mineralogy than Pauling's (1929) electrostatic valence rule, proposed more than half a century ago but still used today to characterize the relative strengths of bonds and local charge balance in silicates. The rule postulates that the sum of strengths of the electrostatic bonds, p_0, to each oxygen atom from the adjacent metal atoms in a silicate should exactly or nearly equal 2.0 in order to saturate the valency of the atom. Through the years, not only has this rule been useful in restricting plausible structure types for a substance, but it has also been found to be an important aid in the determination of crystal structures. When first proposed, it was found to be exactly or nearly completely satisfied in a variety of silicates. However, as more and more silicate structures were determined, more and more violations were reported. Smith (1953), for example, found in a reexamination of the melilite structure that the p_0 value of one of the oxygen atoms departs by as much as 20 percent from 2.0. Following the discovery that a positive correlation exists between R(SiO) and p_0, he went on to make the important postulate that the variations in R(SiO) can serve to alter the bond strengths so that the valence of each oxygen atom in the structure is effectively saturated by the strengths of the bonds reaching it.

In 1970, Baur reexamined this correlation and found that about half the variation in R(SiO) for nearly 300 SiO bonds from a wide variety of silicates could be described in terms of a linear dependence on p_0. Later, Phillips, Ribbe and Gibbs (1973) also found that about half of the variation of R(TO) (T = Si, Al) in the feldspar, anorthite, could be similarly described. But they also found that about 40 percent of the R(TO) variations in the feldspar could be described in terms of the SiOAl angle with shorter bonds tending to involve wider angles (see also Brown, Gibbs and Ribbe, 1969).

To ascertain whether both p_0 and f_s make a significant contribution to the regression sum of squares when considered in the presence of each other, Geisinger, Swanson, Meagher and Gibbs (unpublished) completed a multiple linear regression analysis of R(SiO) as a function of p_0 and f_s for more than 130 SiO bond lengths in eleven tectosilicates, including anorthite. The analysis yielded the equation

$$\mathrm{R(SiO)} = 1.49 + 0.10p_0 - 0.16f_s \qquad (17)$$

Not only do statistical tests indicate that both p_0 and f_s make a significant contribution to the regression sum of squares, but also the resultant multiple correlation coefficient indicates that about 70 percent of the total variance in R(SiO) may be accounted for by its regression on p_0 and f_s. When the AlO bond length data for the tectosilicates were included in the regression analysis, the calculation yielded the equation

$$\mathrm{R(TO)} = 1.49 + 0.10p_0 - 0.16f_s + 0.132x \qquad (18)$$

where x was set equal to 0.0 and 1.00 for SiO and AlO bonds, respectively. Note that the regression coefficients for p_0 and f_s are identical in both (17) and (18), indicating that both data sets may be commingled and treated as a single population. The fact that they are identical suggests that the bonding forces that govern R(TO) in the tectosilicates are very similar irrespective of whether a tetrahedral group contains either Si or Al. As expected, the coefficient of x in (18) is equal to the difference between the crystal radii of four-coordinate Al and Si published by Shannon and Prewitt (1969).

The observed tetrahedral bond lengths, $\mathrm{R(TO)_{obs.}}$, used in the regression analysis are plotted in Figure 15b against $\mathrm{R(TO)_{calc.}}$, calculated with (18) using the p_0, f_s and x values observed for the more than 200 bond lengths employed in the analysis. Although the agreement is not perfect (some of the bond lengths depart by as much as 0.03Å from the 45° line of perfect agreement), equation (18) orders the experimental bond lengths rather well in conformity with the line drawn in Figure 15b.

As the bond lengths and angles generated for the

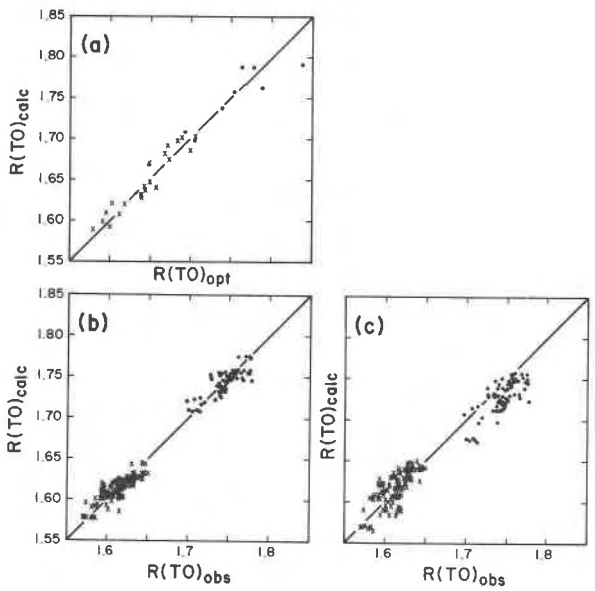

Fig. 15. Tetrahedral TO (T = Si, Al) bond lengths, $R(TO)_{calc.}$, calculated as a linear combination of bond strength sum, p_o, the fraction of *s*-character of the bridging oxygen atom, f_s, and the Al-content, x, of the tetrahedron containing the bond. (a) The tetrahedral bond lengths, $R(TO)_{calc.}$, calculated using equation (19) and the p_o and f_s values for a number of molecules *versus* their optimized bridging bond lengths, $R(TO)_{opt.}$; (b) The tetrahedral bond lengths, $R(TO)_{calc.}$, calculated with equation (18) using the observed p_o and f_s values for eleven tectosilicates (α-quartz, low cristobalite, coesite, anorthite, low albite, low microcline, low cordierite, paracelsian, slawsonite, reedmergnerite and danburite) *versus* the bridging bond lengths, $R(TO)_{obs.}$, observed for these minerals (The Al and Si atoms were assumed to be ordered in each of these phases); (c) The tetrahedral bond lengths, $R(TO)_{calc.}$, calculated with equation (19) using the observed p_o and f_s values for the eleven tectosilicates versus their observed bridging bond lengths, $R(TO)_{obs.}$. The solid lines drawn on each scatter diagram represent lines of perfect agreement. (After Geisinger and Gibbs, 1981b.)

TOT groups in the silicate and siloxane molecules described in this report and elsewhere (Meagher *et al.*, 1980; Swanson *et al.*, 1980; Gibbs *et al.*, 1981) agree rather well with those in solid silicates and siloxanes, Geisinger *et al.* (unpublished) completed a multiple linear regression analysis of R(TO) as a function of p_0, f_s and x for more than 25 molecules whose bond lengths and angles had been optimized with STO-3G basis functions. As in the case of the tectosilicates, each variable was indicated to make a significant contribution to the regression sum of squares. Also, the optimized bond lengths, $R(TO)_{opt.}$, used in the regression analysis were observed to be highly correlated ($R^2 = 0.94$) with those calculated for the molecules as evinced by Fig. 15a. As a matter of fact, when the equation

$$R(TO) = 1.64 + 0.08p_0 - 0.41f_s + 0.11x \quad (19)$$

obtained in the regression analysis is evaluated using the p_0, f_s and x values for each TO bond in the tectosilicates, the resulting $R(TO)_{calc.}$ values serve to rank the observed bond lengths fairly well (Fig. 15c). The ability of this equation to rank the observed bond lengths is additional evidence that the forces governing the shape of the SiOT group in a molecule and a tectosilicate are virtually the same, notwithstanding the long range Madelung potential of the solid.

An examination of the regression coefficients of (18) indicates that R(TO) increases with decreasing f_s (with narrowing of the SiOT angle) and with increasing p_0. Inasmuch as the expected distance of a 2*p*-electron from the oxygen atom nucleus is greater than that of a corresponding 2*s*-electron, the increase of R(TO) with decreasing f_s is anticipated. In other words, R(TO) should increase with decreasing f_s because the effective radius of the oxygen atom is expected to increase linearly with its state of hybridization in the order $sp < sp^2 < sp^3$ (Dewar and Schmeising, 1960; Brown and Gibbs, 1969; Newton and Gibbs, 1980).

The linear dependence between bond length and p_0 is well-documented for a number of oxides, including phosphates, sulfates, borates, silicates and aluminates (Baur, 1970; Swanson *et al.*, 1980; Geisinger and Gibbs, 1981b). Interestingly, even though Si is more electronegative and effectively smaller than Al, both R(SiO) and R(AlO) exhibit about the same linear dependence on p_0 within the experimental error. This is in contrast with the observation by Lager and Gibbs (1973) that the dependence seems to be better developed for the most electronegative metal atoms. The dependence of R(SiO) and R(AlO) on p_0 has been analyzed by Meagher et al. (1980) and Swanson *et al.* (1980) both of whom optimized the geometries of a number of molecules with bridging SiOSi, SiOAl, and AlOAl groups and with p_0 values ranging between 1.50 and 3.00. Their analyses indicate that the bond length variations in the molecules are linearly dependent upon p_0 and that the R(TO) *versus* p_0 correlations generated for the molecules duplicate the trends recorded for various silicates (Fig. 16) by Baur (1970) and Geisinger *et al.* (unpublished). Population analyses for several of these molecules indicate that the bond-length dependence on p_0 is related to a redistribution of the charge density in the bonds

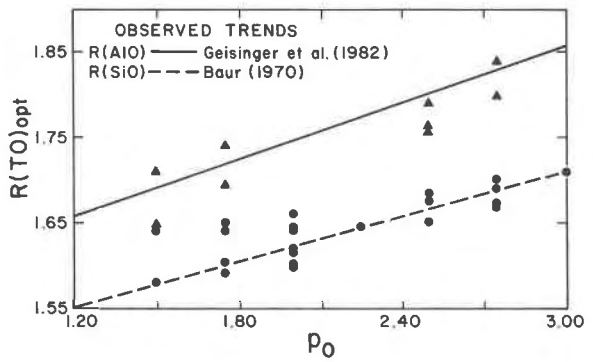

Fig. 16. Bridging tetrahedral TO (T = Al, Si) bond lengths, R(TO), optimized for a number of molecules *versus* the bond strength sums, p_o, of the bridging oxygen atoms. The R(SiO) and R(AlO) data are plotted as bullets and triangles, respectively The lines drawn through the two trends were obtained in regression analyses of observed tetrahedral AlO and SiO bond length data *versus* p_o for a large number of silicates. (After Geisinger and Gibbs, 1981b.)

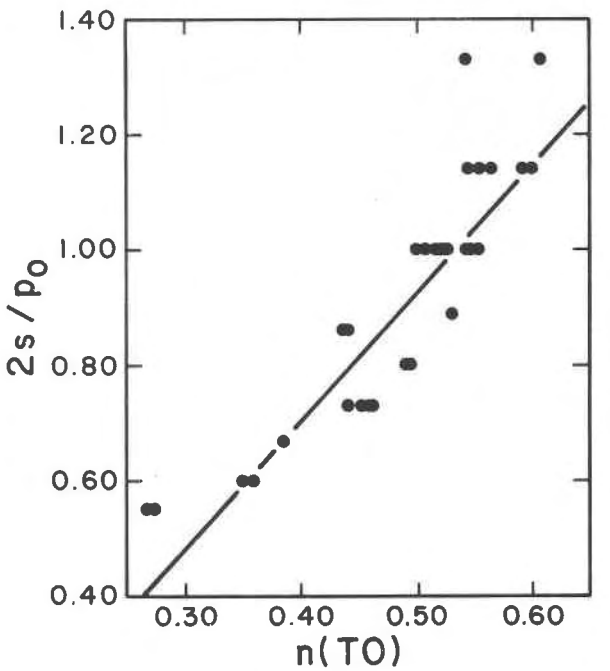

Fig. 17. A scatter diagram of the normalized bond strengths, $2s/p_o$, for the bridging SiO and AlO bonds in more than 25 molecules *versus* the Mulliken bond overlap populations calculated with the optimized bridging bond lengths and angles. The quantity s is the Pauling electrostatic bond strength, and p_o is the bond strength sum of the bridging oxygen atom. (After Geisinger and Gibbs, 1981b.)

(Geisinger and Gibbs, 1981b). In particular, as p_0 increases, the charge density build-up in the bonds reaching the bridging oxygen may be reduced as the charges on the Si atoms increase, implying an increase in the overall ionicity of the system. This is expected to lead to an overall weakening and a concomitant lengthening of the bonds to the oxygen atoms. In addition, when the electrostatic bond strengths for each of the SiO and AlO bonds are multiplied by $2.0/p_0$, a well-developed correlation obtains between the resulting bond strengths and the Mulliken overlap populations calculated for the optimized bond lengths of the molecules (Fig. 17). Thus, it is apparent that p_0 is a measure of bond strength irrespective of whether the bonds are considered to be ionic, covalent or some resonating structure in between the two extremes.

The Pauling concept of bond strength

As we have seen in the earlier sections of this report, the application of molecular quantum chemistry to bonding problems in silicates has provided new and valuable insights into bond length and angle variations, charge density distributions and the elastic properties of the bonds. In this section, we will examine two sets of first- and second-period bond strength-bond length curves generated for the hydroxyacid molecules in Table 3 (Gibbs and Newton, in prep.). In addition to mimicking the well known Brown-Shannon curves (1973), the theoretical curves will be found capable of reproducing the Pauling (1929) bond strengths, s (= the valence of a metal atom divided by its coordination number), of the bonds in the molecules. Also, a Mulliken population analysis will show that s is linearly correlated with bond overlap population in agreement with earlier assertions that s may be equated with bond number (Gibbs *et al.*, 1972; Brown and Shannon, 1973; Lager and Gibbs, 1973).

Bond strength–bond length curves

A number of relations have been proposed between bond strength and bond length (see Brown and Shannon (1973) for an excellent review of these relations). One of the simplest ones is presented in Figure 18a where ln(s) is plotted against ln(R(XO)) for first and second-period metal atoms, X (Gibbs and Newton, in prep.). The R(XO) values used in preparing these plots were generated with the Shannon–Prewitt (SP) crystal radii (1969), assuming an oxide ion radius of 1.22Å. Inasmuch as the SP radii were obtained from accurate bond length data from a large variety of crystal structures, the R(XO) values used in the plots may be taken as accurate

Table 3: Optimized bond lengths, R(XO), for various hydroxy-acid molecules; s is the electrostatic bond strength of the XO bond and $s_{calc.}$ are the bond strengths calculated with equation (21) and the theoretical constants given in the final section of this report

Molecule	R(XO)	s	$s_{calc.}$
First period XO bonds			
$CO(OH)_2$	1.33	1.33	1.26
$B(OH)_3$	1.36	1.00	1.08
$B(OH)_3(OH_2)$	1.46	0.75	0.77
$Be(OH)_2(OH_2)$	1.51	0.67	0.65
$Be(OH)_2(OH_2)_2$	1.58	0.50	0.51
$Li(OH)(OH_2)_3$	1.80	0.25	0.25
$Li(OH)(OH_2)_5$	1.97	0.17	0.16
Second period XO bonds			
$Si(OH)_4$	1.65	1.00	1.05
$Al(OH)_3$	1.67	1.00	0.96
$Al(OH)_3(OH)$	1.72	0.75	0.77
$Si(OH)_4(OH_2)_2$	1.76	0.67	0.65
$Mg(OH)_2(OH_2)$	1.78	0.67	0.60
$Al(OH)_3(OH_2)_3$	1.79	0.50	0.58
$Mg(OH)_2(OH_2)_2$	1.83	0.50	0.49
$Mg(OH)_2(OH_2)_4$	1.91	0.33	0.36
$Na(OH)(OH_2)_2$	1.99	0.33	0.27
$Na(OH)(OH_2)_3$	2.02	0.25	0.24
$Na(OH)(OH_2)_5$	2.07	0.17	0.20

estimates of the XO bond lengths for various coordination polyhedra in oxide solids. In an effort to reproduce the correlations in Figure 18a, Gibbs and Newton (in prep.) undertook a series of molecular orbital calculations for a variety of hydroxyacid molecules (Table 3) with three-, four- and six-coordinate metal atoms to explore the extent to which the ln(R(XO)) values for the molecules might be linearly correlated with ln(s) and to see whether the overlap populations, n(XO), of the optimized XO bonds correlate with the electrostatic bond strengths. The protons used to neutralize the molecules in Table 3 were placed at 0.96Å from the oxygen atoms and the XOH angles were fixed at 109.47° as described earlier, for instance, for the $Si(OH)_4(OH_2)_2$ molecule displayed in Figure 4b. In the calculations, the XO bonds of each molecule were treated as though they were equivalent while the optimized R(XO) values were found by fitting a three-point parabola to each potential energy curve in close proximity to the energy minimum. When Gibbs and Newton (in prep.) plotted the resulting ln(R(XO)) values against ln(s), two linear trends emerged (Fig. 18b) like those displayed in Figure 18a. Unlike the two empirical trends, which parallel one another, the theoretical trends possess slightly steeper slopes and show a slight divergence. On the other hand, the empirical ones are identical in both slope and intercept with those reported by Brown and Shannon (1973) which were obtained by requiring the bond strength sums reaching the metal atoms in more than 400 crystals to equal the formal valences on these atoms.

As the trends in Figure 18 are highly linear, each may be modeled by the linear equation

$$\ln(s) = a + b\ln(\mathrm{R(XO)}). \qquad (20)$$

And, if we set $a = N\ln(R)$ and $b = -N$, where N and R are constants, (20) becomes

$$\ln(s) = N\ln(R) - N\ln(\mathrm{R(XO)}),$$

$$\ln(s) = \ln(\mathrm{R(XO)}/R)^{-N},$$

and we have

$$s = (\mathrm{R(XO)}/R)^{-N}. \qquad (21)$$

This equation corresponds with an expression proposed by Donnay and Allman (1970) and independently refined by Pyatenko (1973) and Brown and Shannon (1973) for modeling bond strength versus bond length variations. An analysis of the regression equations fitted to the data in Figure 18 yields

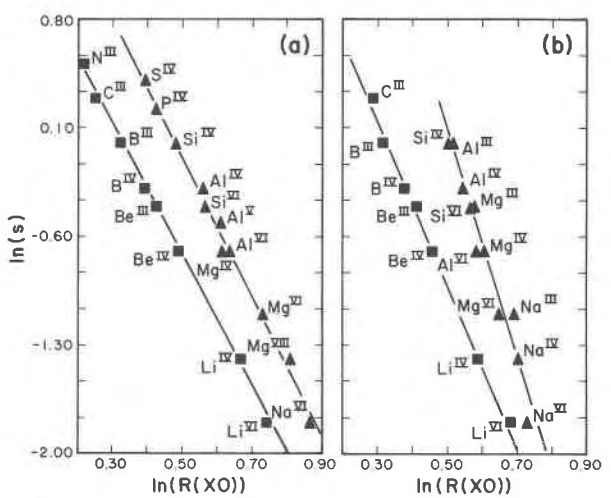

Fig. 18. Plots of ln(s) *versus* ln(R(XO)) where s is the Pauling bond strength and R(XO) is the interatomic separation between the first and second row cation X and an oxygen anion. (a) ln(s) *versus* ln(R(XO)) where R(XO) is the sum of the crystal radii of an X cation and the oxygen anion. (These plots were prepared with those X cations whose radii were considered to be accurate by Shannon and Prewitt (1969); cation radii tagged with a question mark were omitted); (b) ln(s) versus ln(R(XO)) where R(XO) is the bond length optimized for each of the $H_{2n-z}X^zO_n$ molecules in Table 3. (After Gibbs and Newton, in preparation.)

the following least-squares estimates of R and N (Gibbs and Newton, in prep.).

	FIRST PERIOD		SECOND PERIOD[5]	
	R	N	R	N
Empirical SP-R(XO):	1.38	4.2	1.62	4.3
Theoretical R(XO):	1.39	5.2	1.66	7.3

When equation (21) is mapped out for each R and N pair above, it is apparent that the theoretical bond strength versus bond length curves are somewhat steeper than those obtained with the SP radii (Fig. 19). Despite this difference, when the s values for the hydroxyacid molecules in Table 3 are calculated with the theoretical equations, they agree to within 0.04 units, on the average, with Pauling's values (Table 3). Finally, when the bond overlap populations calculated for the molecules are plotted against Pauling bond strength (Fig. 20), a strong correlation ($r^2 = 0.98$) is observed in agreement with the assertion that s can be equated with bond number (Gibbs *et al.*, 1972). Thus, we consider the bond length versus bond strength curves of Donnay and Allman (1970), Pyatenko (1973) and Brown and Shannon (1973) to have the same meaning and significance as the well known carbon–carbon bond length *versus* bond number curves published for the hydrocarbons by Pauling (1960) and Coulson (1961). Even though the Pauling bond strength has its origin in the ionic model, the trend in Figure 20 indicates that is a direct measure of the strength of a bond regardless of whether the bond is considered to be ionic or covalent, the larger the value of s, the shorter the bond. Moreover, when the bond lengths in an oxide are taken into account, the Brown–Shannon curves have been shown to generate bond strengths that sum to values close to the formal valences on the atoms in conformity with Pauling's electrostatic valence principle. Finally, the reproduction of the bond strength versus bond length curves with molecular orbital theory has established a connection between experiment and theory

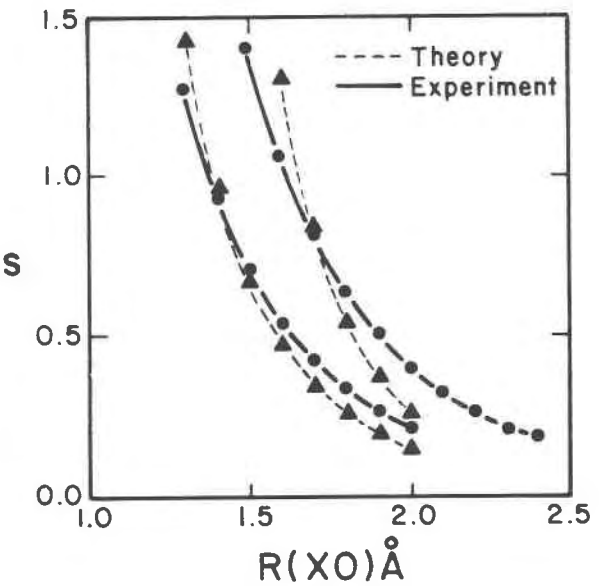

Fig. 19. Theoretical and experimental bond strength–bond length curves. (After Gibbs and Newton, in preparation.)

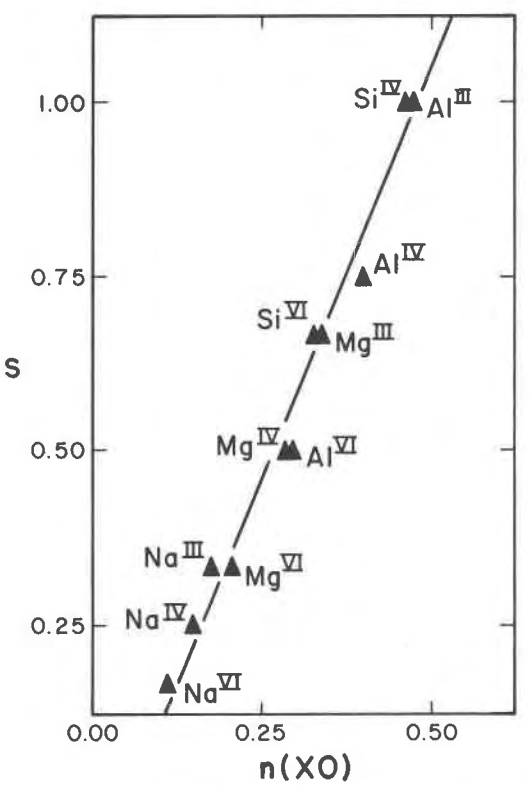

Fig. 20. The Pauling bond strength s *versus* the average Mulliken bond overlap population of the XO bonds for the molecules listed in Table 3 (after Gibbs and Newton, in prep.).

[5] Employing a STO-3G* basis set with d-type AO's on Si, Chakoumakos and Gibbs (1981b) have since derived the theoretical equation $s = (R(XO)/1.59)^{-3.8}$, using the SiO bond lengths optimized for three hydroxyacid molecules with 4-, 6- and 8-coordinated Si. Although this equation is based on only three bond lengths, it agrees very well with an empirical equation $s = (R(XO)/1.62)^{-4.3}$ derived by Brown and Shannon (1973). Note that the constants derived by them are virtually the same as those derived here with the Shannon–Prewitt crystal radii.

and has provided a quantum mechanical underpinning for Pauling's second rule (Pauling, 1929).

Some concluding remarks

Important advances have been made in the last few years in generating structures, heats of formation, electron density distributions and equations of state for a variety of simple solids, using the principles and methods of quantum mechanics. Bukowinski (1980, 1981), for example, has successfully calculated equations of state and electronic densities for the minerals periclase, MgO, and lime, CaO, using a self-consistent symmetrized augmented plane wave method. Clearly the success of these calculations augurs well for establishing new standards for future high pressure studies of minerals of geophysical interest and for furthering our understanding of the deep interior of the earth. Equally important in the field of solid state physics, Phillips (1973) and Cohen (1973), for example, have used the pseudopotential method to improve our understanding of structures, stabilities, electron charge distributions and compressibilities of a variety of simple solids, consisting of either one, two or three atom types (see Chapters 1–6, O'Keeffe and Navrotsky, 1981). In addition, Chelikowsky and Schluter (1977) have used the method to generate the band gap, the photoemission spectra and the pseudocharge density distribution for α-quartz. Notwithstanding the efficacy of these powerful methods, they have, for the most part, been limited by computational effort (*i.e.*, computer costs) to a relatively simple class of structures like diamond, rock salt and wurtzite and as such have yet to be applied globally in calculating bond length and angle variations, deformation densities and force constants for such important rock-forming minerals as the silica polymorphs, the feldspars, and the biopyriboles. Until these calculations are affordable and forthcoming, we suggest that molecular orbital calculations on representative molecules can be used to improve our understanding of the solid state properties and the nature of the bonding forces in these rock-forming minerals.

As described in this report, a variety of recent *ab initio* calculations on various siloxane and silicate molecules has given a fairly good account of the bond length and angle variations in solid siloxanes and silicates. Besides providing valuable data on the charge density distribution, the compressibility, the polymorphism and the glass-forming tendencies of silica, the calculations have also shed light on the question of why silicates exhibit such a large assortment of structure types. They have also proven useful in interpreting the bond length and angle variations and the glass-forming tendencies of silicates with SiOSi, SiOAl, SiOB and SiOBe groups. By reproducing the Brown–Shannon bond length–bond strength curves, the calculations have also provided a quantum mechanical underpinning of Pauling's electrostatic valence principle by showing that the strength of a bond is dependent on bond length to the extent that the valence on each oxygen atom in a structure is effectively saturated by the electrostatic valences of the bonds reaching it as postulated by Smith (1953).

In light of the successful application of these calculations to silicates, we are forced to conclude that the bond length and angle variations, the local force field and the deformation densities in silicates are governed in large part by the local atomic arrangement of a solid. Moreover, the success of a large number of semi-empirical molecular orbital calculations in ranking the bond lengths and angles for a variety of phosphates, sulfates, germanates, *etc.*, indicates that this conclusion may hold for a relatively large class of inorganic solids (Lager and Gibbs, 1973; Tossell and Gibbs, 1977; Louisnathan, Hill and Gibbs, 1977; Hill, Louisnathan and Gibbs, 1977). In fact, Bullett (1980) has reached a similar conclusion in a review of the tight-binding method and its ability to generate equilibrium cell dimensions, directional Compton profiles, and local densities of state for a variety of semiconductors and transition metals.

During the coming years, we believe that molecular orbital theory will provide a great deal of new and valuable mineralogical information about the principles governing the formation of various structure types as well as identifying systematic relationships between structure and physical properties. In particular, we suggest that the theory will provide new insight into such physico-chemical processes as sorption, diffusion and catalysis in the zeolite minerals, ion exchange and order-disorder transformations in the feldspars, chemical reactions and reaction paths in silicate minerals and glasses, the cleavage mechanism of the disiloxy group by water and its bearing on the reaction of silicate minerals and glasses with water,dissolution mechanisms and the self-condensation and hydrolysis of such materials as monosilicic acid (Gibbs, Meagher, Smith and Pluth, 1977b; Mortier, Geerlings, Van Alsenoy and Figeys, 1979; DeJong and Brown, 1980b;

Sauer, Hobza and Zahradnik, 1980; Hass and Mezey, 1981; Chakoumakos and Gibbs, 1981a).

In concluding this report, we suggest that mineralogists can no longer look upon the application of quantum mechanical theory to mineralogical problems as an object of mere curiosity. The insight afforded by the theory, the understanding provided by its application as well as its ability to generate data for unknown quantities not amenable to direct measurement are compelling and cogent reasons for acquiring some knowledge of the theory. However, if we persist in studying minerals solely by conventional methods, then we can expect to forfeit a segment of our field of research and expertise to the chemists and physicists who are being attracted into the field of quantum mineralogy by its many important and challenging problems.

Acknowledgments

I owe a debt of thanks to Professor E. P. Meagher, Dr. Marshall D. Newton, my students and colleagues for sharing with me their ideas on the meaning and significance of the calculations and the results discussed in this report. I am particularly indebted to Marshall Newton for teaching me a number of important concepts in theoretical quantum chemistry and for showing patience with me while I struggled to assimilate the subject. I wish to thank Professors F. D. Bloss, G. E. Brown, Jr., M. S. T. Bukowinski, J. K. Burdett, G. C. Grender, A. Lasaga, A. Navrotsky, P. H. Ribbe, J. D. Rimstidt, M. A. Spackman, J. W. Viers and D. R. Wones, as well as each of my collaborators for their valuable remarks in reviewing this report. However, they are neither responsible for my errors nor my infelicities. I am very grateful to VPI for promoting the growth and development of an excellent University Computer Center and for contributing generous sums of monies to help defray the computing costs incurred in our molecular orbital calculations. Ramonda Haycocks, a secretary of exceptional talent and ingenuity, prepared the script file of the report, transforming my handwritten rough drafts into immaculate typescript. Professor Robert F. Stewart and Dr. Mark A. Spackman of the Chemistry Department at Carnegie Mellon University are thanked for providing me with a deformation map for SiO calculated with Hartree-Fock wavefunctions and for calculating the map for stishovite in Figure 6a. Professor Alan Clifford of the Chemistry Department at VPI is thanked for helpful advice on the nomenclature of the molecules examined in the study. I thank Sharon Chiang and Martin Eiss for drafting the figures. I am especially indebted to the National Science Foundation for supporting this work with Grant EAR 77-23114 awarded to Professor P. H. Ribbe and myself to study bonding in minerals.

References

Adams, T., Debaerdemacker, T. and Thewalt, U. (1979) Complexes of six-coordinate silicon. Collected Abstracts, 5th European Crystallographic Meeting, Copenhagen, 32S.

Almenningen, A., Bastiansen, O., Ewing, V., Hedberg, K. and Traetteberg, M. (1963) The molecular structure of disiloxane, $(SiH_3))_2O$. Acta Chemica Scandinavica, 17, 2455–2460.

Bader, R. F. W., Keeveny, P. E. and Cade, J. (1967) Molecular charge distributions and chemical binding. II. First-row diatomic hydrides. American Journal of Chemical Physics, 47, 3381–3402.

Barrow, M. J., Ebsworth, E. A. V. and Harding, M. M. (1979) The crystal and molecular structures of disiloxane (at 108K) and hexamethyldisiloxane (at 148 K). Acta Crystallographica, B35, 2093–2099.

Bass, J. D., Liebermann, R. C., Weidner, D. J. and Stephen, J. F. (1981) Elastic properties from acoustic and volume compression experiments. Physics of the Earth and Planetary Interiors, 25, 140–158.

Baur, W. H. (1970) Bond length variation and distorted coordination polyhedra in inorganic crystals. Transactions of the American Crystallographic Association, 6, 125–155.

Baur, W. H. (1971) The prediction of bond length variations in silicon-oxygen bonds. American Mineralogist, 56, 1573–1599.

Baur, W. H. (1977) Silicon–oxygen bond lengths, bridging angles, SiOSi and synthetic low tridymite. Acta Crystallographica, B33, 2615–2619.

Baur, W. H. (1978) Variation of mean Si–O bond lengths in silicon–oxygen tetrahedra. Acta Crystallographica, B34, 1751–1756.

Binkley, J. S., Whiteside, R., Hariharan, P. C., Seeger, R., Hehre, W. J., Lathan, W. A., Newton, M. D., Ditchfield, R. and Pople, J. A. (1978) Gaussian 76: an *ab initio* molecular orbital program. Quantum Chemistry Program Exchange, Bloomington, IN.

Boys, S. F. (1950) Electronic wave functions I. A general method of calculation for the stationary states of any molecular system. Proceedings of the Royal Society, London, A200, 542–554.

Brown, G. E. and Gibbs, G. V. (1969) Oxygen coordination and the Si-O bond. American Mineralogist, 54, 1528–1539.

Brown, G. E. and Gibbs, G. V. (1970) Stereochemistry and ordering in the tetrahedral portion of silicates. American Mineralogist, 55, 1587–1607.

Brown, G. E., Gibbs, G. V. and Ribbe, P. H. (1969) The nature and variation in length of the Si–O and Al–O bonds in framework silicates. American Mineralogist, 54, 1044–1061.

Brown, I. D. and Shannon, R. D. (1973) Empirical bond-strength–bond-length curves for oxides. Acta Crystallographica, A29, 266–282.

Brytov, I. A., Romashchenko, Yu. N. and Shchegolev, B. F. (1979) Electronic structure of the octahedral oxyanions of aluminum and silicon. Translated from Zhurnal Strukturnoi Khimii, 20, No. 2, 227–234.

Bukowinski, M. S. T. (1980) Effect of pressure on bonding in MgO. Journal of Geophysical Research, 85, 285–292.

Bukowinski, M. S. T. (1981) Pressure effects on bonding in CaO: Comparison with MgO. Journal of Geophysical Research, 87, 303–310.

Bullett, D. W. (1980) Renaissance of the tight-binding method. In H. Ehrenreich, F. Seitz and D. Turnbull, Eds., Solid State Physics, Vol. 35, Academic Press, New York.

Carksy, P. and Urban, M. (1980) Ab Initio Calculations. Springer-Verlag, New York.

Chakoumakos, B. C. (1981) A Molecular Orbital Study of I. Rings in Silicates and Siloxanes and II. Order-Disorder Isomorphism in Silicate Anions. M.S. Thesis, Virginia Polytechnic Institute and State University, Blacksburg, Virginia.

Chakoumakos, B. C. and Gibbs, G. V. (1981a) The chemical and

physical properties of TOT bonds in beryllosilicates, borosilicates, aluminosilicates and silicates obtained with *ab initio* STO-3G MO theory. (abstr.) EOS, 62, 416.

Chakoumakos, B. C. and Gibbs, G. V. (1981b) Theoretical structural analysis of SiO_2 with the fluorite structure. (abstr.) Geological Society of America Abstracts with Programs, 13, 425.

Chakoumakos, B. C., Hill, R. J. and Gibbs, G. V. (1981) A molecular orbital study of rings in silicates and siloxanes. American Mineralogist, 66, 1237–1249.

Chelikowsky, J. R. and Schluter, M. (1977) Electron states in α-quartz: A self-consistent pseudopotential calculation. Physical Review, B15, 4020–4029.

Cohen, M. L. (1973) Electronic charge densities in semiconductors. Science, 179, 1189–1195.

Collins, G. A. D., Cruickshank, D. W. J. and Breeze, A. (1972) Ab initio calculations on the silicate ion, orthosilicic acid and their $L_{2,3}$ X-ray spectra. Journal of the Chemical Society, Faraday Transactions, 68, 1189–1195.

Collins, J. B., Schleyer, P. von R., Binkley, J. S. and Pople, J. A. (1976) Self-consistent molecular orbital methods. XVII. Geometries and binding energies of second-row molecules. A comparison of three basis sets. Journal of Chemistry and Physics, 64, 5142–5151.

Coulson, C. A. (1961) Valence. Oxford University Press, London.

Coulson, C. A. (1973) The Shape and Structure of Molecules. Clarendon Press, Oxford.

Da Silva, J. R. G., Pinatti, D. G., Anderson, G. E. and Rudee, M. L. (1975) A refinement of the structure of vitreous silica. Philosophical Magazine, 713–717.

De Jong, B. H. W. S. and Brown, G. E. (1980a) Polymerization of silicate and aluminate tetrahedra in glasses, melts, and aqueous solutions—I. Electronic structure of $H_6Si_2O_7$, $H_6AlSiO_7^{1-}$, and $H_6Al_2O_7^{2-}$. Geochimica et Cosmochimica Acta, 44, 491–511.

DeJong, B. H. W. S. and Brown, G. E. (1980b) Polymerization of silicate and aluminate tetrahedra in glasses, melts and aqueous solutions—II. The network modifying effects of Mg^{2+}, K^+, Na^+, Li^+, H^+, OH^-, F^-, Cl^-, H_2O, CO_2 and H_3O^+, Geochimica et Cosmochimica Acta, 44, 1627–1642.

Dewar, M. J. S. (1969) The Molecular Orbital Theory of Organic Chemistry. McGraw-Hill, New York.

Dewar, M. J. S. and Schmeising, H. N. (1960) Resonance and conjugation-II. Factors determining bond lengths and heats of formation. Tetrahedron, 11, 96–120.

Donnay, G. and Allmann, R. (1970) How to recognize O^{2-}, OH^-, and H_2O in crystal structures determined by X-rays. American Mineralogist, 55, 1003–1015.

Downs, J. W. (1980) Bonding in Beryllosilicates: The charge Density of Euclase $AlBeSiO_4(OH)$ and Molecular Orbital Studies of Beryllium Oxyanions. M.S. Thesis, Virginia Polytechnic Institute and State University, Blacksburg, Virginia.

Downs, J. W. and Gibbs, G. V. (1981) The role of the BeOSi bond in the structures of beryllosilicate minerals. American Mineralogist, 66, 819–826.

Downs, J. W., Hill, R. J., Newton, M. D., Tossell, J. A. and Gibbs, G. V. (1982) Theoretical and experimental charge distributions in euclase and stishovite. In P. Coppens and M. Hall, Eds., Electron Distributions and the Chemical Bond, in press, Plenum Press, New York.

Durig, J. R., Flanagan, M. J. and Kalasinsky, V. F. (1977) The determination of the potential function governing the low frequency bending mode of disiloxane. Journal of Chemical Physics, 66, 2775–2785.

Earley, J. E., Fortnum, D., Wojcicki and Edwards, J. O. (1959) Constitution of aqueous oxyanions: Perrhenate, tellurite and silicate ions. Journal of the American Chemical Society, 81, 1295–1301.

Edge, R. A. and Taylor, H. F. W. (1971) Crystal structure of thaumasite, $Ca_3Si(OH)_6 \cdot 12H_2O$ $(SO_4)(CO_3)$. Acta Crystallographica, B27, 594–601.

Engelhardt, G., Zeigan, D., Jancke, H., Hoebbel, D. and Wieker, W. (1975) Zur abhangigkeit det struktur der silicatanionen in wassrigen natriumsilicatlosungen vom Na:Si verhaltnis. Zeitschrift für Anorganische und Allgemeine Chemie, 418, 17–28.

Ernst, C. A., Allred, A. L., Ratner, M. A., Newton, M. D., Gibbs, G. V., Moskowitz, J. W. and Topiol, S. (1981) Bond angles in disiloxane: A pseudo-potential electronic structure study. Chemical Physics Letters, 81, 424–429.

Flynn, J. J. and Boer, F. P. (1969) Structural studies of hexacoordinate silicon. Tris(o-phenylenedioxy)siliconate. Journal of the American Chemical Society, 91, 5756–5761.

Freund, E. (1973) Etude par spectroscopie Raman-laser des solutions aqueuses de silicates de sodium. II. Interpretation des spectres. Bulletin de la Société Chimique de France, 7–8, 2244–2249.

Geisinger, K. L. and Gibbs, G. V. (1981a) SiSSi and SiOSi bonds in molecules and solids: A comparison. Physics and Chemistry of Minerals, 7, 204–210.

Geisinger, K. L. and Gibbs, G. V. (1981b) STO-3G molecular orbital (MO) calculated correlations of tetrahedral SiO and AlO bridging bond lengths with p_o and f_s. (abstr.) Geological Society of America Abstracts with Programs, 13, 458.

Ghose, S., Wang, C., Ralph, R. L. and McMullan, R. K. (1980) Enstatite, $Mg_2Si_2O_6$: Charge density distribution by X-ray and neutron diffraction and the compressibility of the crystal structure at 21 kbar. Collected Abstracts, International Mineralogical Association, 12th General Meeting, Orleans, France, 48–49.

Gibbs, G. V., Hamil, M. M., Louisnathan, S. J., Bartell, L. S. and Yow, H. (1972) Correlations between Si–O bond length, Si–O–Si angle and bond overlap populations calculated using extended Huckel molecular orbital theory. American Mineralogist, 57, 1578–1613.

Gibbs, G. V., Louisnathan, S. J., Ribbe, P. H. and Phillips, M. W. (1974) Semiempirical molecular orbital calculations for the atoms of the tetrahedral framework in anorthite, low albite, maximum microcline and reednergnerite. In W. S. MacKenzie and J. Zussman, Eds., The Feldspars, p. 49–67. Manchester University Press, Manchester.

Gibbs, G. V., Prewitt, C. T. and Baldwin, K. J. (1977a) A study of the structural chemistry of coesite. Zeitschrift für Kristallographie, 145, 108–123.

Gibbs, G. V., Meagher, E. P., Smith, J. V. and Pluth, J. J. (1977b) Molecular orbital calculations for atoms in the tetrahedral framework of zeolites. In J. R. Katzer, Ed., Molecular Sieves. A.C.S. Symposium Series, No. 40, American Chemical Society, New York.

Gibbs, G. V., Hill, R. J., Ross, F. K. and Coppens, P. (1978) Net charge distributions and radial dependences of the valence electrons on the Si and O atoms in coesite. (abstr.) Geological Society of America Abstracts with Programs, GAC/MAC vol.

3, 407.

Gibbs, G. V., Meagher, E. P., Newton, M. D. and Swanson, D. K. (1981) A comparison of experimental and theoretical bond length and angle variations for minerals, inorganic solids, and molecules. In M. O'Keeffe and A. Navrotsky, Eds., Structure and Bonding in Crystals, Vol. 1. p. 195–225. Academic Press, New York.

Gilbert, T. L., Stevens, W. J., Schrenk, H., Yoshimine, M. and Bagus, P. S. (1973) Chemical bonding effects in the oxygen Kα X-ray emission bands of silica. Physical Review, B8, 5977–5998.

Glidewell, C., Robiette, A. G. and Sheldrick, G. M. (1970) Gas-phase electron diffraction structure of tetrameric prosiloxane, $(H_2SiO)_4$. Chemical Communications, 1970, 931–932.

Griscom, D. L. (1977) The electronic structure of SiO_2: A review of recent spectroscopic and theoretical advances. Journal of Non-Crystalline Solids, 24, 155–234.

Gupta, A. and Tossell, J. A. (1981) Theoretical study of bond densities, X-ray spectra and electron density distributions in borate polyhedra. Physics and Chemistry of Minerals, 7, 159–164.

Gupta, A., Swanson, D. K., Tossell, J. A. and Gibbs, G. V. (1981) Calculation of bond distances, one-electron energies and electron density distributions in first-row tetrahedral hydroxy and oxyanions. American Mineralogist, 66, 601–609.

Hass, E. C. and Mezey, P. G. (1981) A non-empirical molecular orbital study on Loewenstein's rule and zeolite composition. Journal of Molecular Structure, 76, 389–399.

Hehre, W. J., Stewart, R. F. and Pople, J. A. (1969) Self-consistent molecular-orbital methods. I. Use of Gaussian expansions of Slater-type atomic orbitals. Journal of Chemical Physics, 51, 2657–2664.

Hill, R. J. and Gibbs, G. V. (1979) Variation in d(T–O), d(T $\cdots$ T) and $\angle$TOT in silica and silicate minerals, phosphates and aluminates. Acta Crystallographica, B35, 25–30.

Hill, R. J., Louisnathan, S. J. and Gibbs, G. V. (1977) Tetrahedral bond length and angle in germanates. Australian Journal of Chemistry, 30, 1673–1684.

Hill, R. J., Newton, M. D. and Gibbs, G. V. (1981) A crystal chemical study of stishovite. (abstr.) EOS, 62, 417.

Iler, R. K. (1955) The Colloid Chemistry of Silica and Silicates. Cornell University Press, Ithaca, New York.

Iler, R. K. (1979) The Chemistry of Silica. Wiley, New York.

Johnson, O. (1973) Ionic radii for spherical ions. I. Inorganic Chemistry, 12, 780–785.

Lager, G. A. and G. V. Gibbs (1973) Effect of variations in O–P–O and P–O–P angles in P–O bond overlap populations for some selected ortho- and pyrophosphates. American Mineralogist, 58, 756–764.

Lager, G. A., J. D. Jorgensen and F. J. Rotella (1982) Crystal structural and thermal expansion of α-quartz SiO_2 at low temperatures, J. Applied Physics, in press.

Lasaga, A. C. (1982) Optimization of CNDO for molecular orbital calculations and silicates. Physics and Chemistry of Minerals, 7, 36–46.

Levien, L., Prewitt, C. T. and Weidner, D. J. (1980) Structure and elastic properties of quartz at pressure. American Mineralogist, 65, 920–930.

Liebau, F. (1971) Zur Kristallchemie des sechsfach koordinierten Siliziums. Bulletin Société Francaise de Mineralogie et de Cristallographie, 94, 239.

Liebau, F. (1980) Classification of silicates. In P. H. Ribbe, Ed., Reviews in Mineralogy, vol. 5, Orthosilicates, p. 1–24. Mineralogical Society of America, Washington, D.C.

Louisnathan, S. J., Hill, R. J. and Gibbs, G. V. (1977) Tetrahedral bond length variations in sulfates. Physics and Chemistry of Minerals, 1, 53–69.

McWeeny, R. (1979) Coulson's Valence, 3rd edition. Oxford University Press, Oxford, 435 pp.

Meagher, E. P. and Gibbs, G. V. (1976) A molecular orbital interpretation of bond length variations in the silica polymorphs. Paper presented at the Canadian Crystallographic Conference, McMaster University, Hamilton, Ontario, Canada.

Meagher, E. P., Tossell, J. A. and Gibbs, G. V. (1979) A CNDO/2 molecular orbital study of the silica polymorphs quartz, cristobalite, and coesite. Physics and Chemistry of Minerals, 4, 11–21.

Meagher, E. P., Swanson, D. K. and Gibbs, G. V. (1980) The calculation of tetrahedral Si–O and Al–O bridging bond lengths and angles. (abstr.) EOS, 61, 408.

Meier, R. and Ha, T. K. (1980) A theoretical study of the electronic structure of disiloxane. $(SiH_3)_2O$ and its relation to silicates. Physics and Chemistry of Minerals, 6, 37–46.

Mortier, W. J., Geerlings, P., Van Alsenoy, C. and Figeys, H. P. (1979) A CNDO study of the electronic structure of faujasite type six-rings as influenced by the placement of magnesium and by the isomorphous substitution of aluminum for silicon. Journal of Physical Chemistry, 83, 855–861.

Mulliken, R. S. (1932) Electronic structures of polyatomic molecules and valence. II. General considerations. Physical Review, 41, 49–71.

Mulliken, R. S. (1935) Electronic structures of molecules. XI. Electroaffinity, molecular orbitals and dipole moments. Journal of Chemical Physics, 3, 573–585.

Mulliken, R. S. (1955) Electronic population analysis on LCAO-MO molecular wavefunctions. I. Journal of Chemical Physics, 23, 1833–1840.

Nakajima, Y., Swanson, D. K. and Gibbs, G. V. (1980) Calculation of tetrahedral Si-N bond lengths and angles. (abstr.) EOS, 61, 408.

Newton, M. D. (1981) Theoretical probes of bonding in the siloxyl group. In M. O'Keeffe and A. Navrotsky, Eds., Structure and Bonding in Crystals, vol. 1, Academic Press, New York.

Newton, M. D. and Gibbs, G. V. (1979) A calculation of bond length and angles, force constants, vertical ionization potentials and charge density distributions for the silicate ion in H_4SiO_4, $H_6Si_2O_7$, and H_6Si_2O. (abstr.) EOS, 60, 415.

Newton, M. D. and Gibbs, G. V. (1980) *Ab initio* calculated geometries and charge distributions for H_4SiO_4 and $H_6Si_2O_7$ compared with experimental values for silicates and siloxanes. Physics and Chemistry of Minerals, 6, 221–246.

Newton, M. D., O'Keeffe, M. and Gibbs, G. V. (1980) *Ab initio* calculation of interatomic force constants in $H_6Si_2O_7$ and the bulk modulus of α-quartz and α-cristobalite. Physics and Chemistry of Minerals, 6, 305–312.

Noll, W. (1968) Chemistry and Technology of Silicones. Academic Press, New York.

Oberhammer, H. and Boggs, J. E. (1980) Importance of (p–d)pi bonding in the siloxane bond. Journal of the American Chemical Society, 102, 7241–7244.

O'Keeffe, M. and Navrotsky, A. (1981) Structure and Bonding in Crystals. Academic Press, New York.

Pacansky, J. and Hermann, K. (1978) *Ab initio* SCF calculations on molecular silicon dioxide. Journal of Chemical Physics, 69, 963–967.

Parr, R. G. (1964) The Quantum Theory of Molecular Electronic Structure. W. A. Benjamin, Inc., New York.

Pauling, L. (1929) The principles determining the structure of complex ionic crystals. Journal of the American Chemical Society, 51, 1010–1026.

Pauling, L. (1939) The Nature of the Chemical Bond, 1st ed. Cornell University Press, Ithaca, New York.

Pauling, L. (1948) The modern theory of valency. Journal of the Chemical Society, 1948, 1461–1467.

Pauling, L. (1952) Interatomic distances and bond character in the oxygen acids and related substances. Journal of Physical Chemistry, 56, 361–365.

Pauling, L. (1960) The Nature of the Chemical Bond, 3rd ed. Cornell University Press, Ithaca, New York.

Peterson, R. C. (1980) Bonding in Minerals: I. Charge Density of the Aluminosilicate Polymorphs, and II. Molecular Orbital Studies of Distortions in Layer Silicates. Ph.D. Dissertation, Virginia Polytechnic Institute and State University, Blacksburg, Virginia.

Phillips, J. C. (1973) Bonds and Bands in Semiconductors. Academic Press, New York.

Phillips, M. W., Ribbe, P. H. and Gibbs, G. V. (1973) Tetrahedral bond length variations in anorthite. American Mineralogist, 58, 495–499.

Pople, J. A. (1953) Electron interaction in unsaturated hydrocarbons. Transactions of the Faraday Society, 49, 1375–1385.

Pople, J. A. (1973) Quantum chemistry. Theory of geometries and energies of small molecules. In F. Herman, A. D. McLean and R. K. Nesbet, Eds., Computational Methods for Large Molecules and Localized States in Solids, p. 11–21. Plenum Press, New York.

Pople, J. A. (1977) *A priori* geometry predictions. In H. F. Schaefer, Ed., Modern Theoretical Chemistry, vol. 4, Applications of Electronic Structure Theory, p. 1–27. Plenum Press, New York.

Pople, J. A. and Beveridge, D. L. (1970) Approximate Molecular Orbital Theory. McGraw-Hill, New York.

Pulay, P. (1969) *Ab initio* calculation of force constants and equilibrium geometries in polyatomic molecules. I. Theory. Molecular Physics, 17, 197–204.

Pyatenko, Yu. A. (1973) Unified approach to analysis of the local balance of valences in inorganic structures. Soviet Physics–Crystallography, 17, 677–682.

Ribbe, P. H., Gibbs, G. V. and Hamil, M. M. (1977) A refinement of the structure of dioptase, $Cu_6Si_6O_{18} \cdot 6H_2O$. American Mineralogist, 62, 807–811.

Roothaan, C. C. J. (1951) New developments in molecular orbital theory. Reviews of Modern Physics, 23, 69–89.

Ross, N. L. and Meagher, E. P. (1981) An *ab initio* MO study of $H_6Si_2O_7$ at simulated high pressure. (abstr.) EOS, 62, 416.

Sauer, J. and Zurawski, B. (1979) Molecular and electronic structure of disiloxane. An *ab initio* MO study. Chemical Physics Letters, 65, 587–591.

Sauer, J., Hobza, P. and Zahradnik, R. (1980) Quantum chemical investigation of interaction sites in zeolites and silica. Journal of Physical Chemistry, 84, 3318–3326.

Schaefer, N. F. (1977) Modern Theoretical Chemistry, vol. 4, Applications of Electronic Structure Theory. Plenum Press, New York.

Shannon, R. D. and Prewitt, C. T. (1969) Effective ionic radii in oxides and fluorides. Acta Crystallographica, B25, 925–946.

Shannon, R. D., Chenavas, J. and Joubert, J. C. (1975) Bond strength considerations applied to cation coordination in normal and high-pressure oxides. Journal of Solid State Chemistry, 12, 16–30.

Shavitt, I. (1963) The Gaussian function in calculations of statistical mechanics and quantum mechanics. In Alder, Ed., Methods in Computational Physics, vol. II, p. 1–45. Academic Press, New York.

Slater, J. C. (1972) Symmetry and Energy Bands in Crystals. Dover Publications, New York.

Smith, J. V. (1953) Reexamination of the crystal structure of melilite. American Mineralogist, 38, 643–661.

Smith, J. V. and Bailey, S. W. (1963) Second review of Al–O and Si–O tetrahedral distances. Acta Crystallographica, 16, 801–810.

Spackman, M. A., Stewart, R. F. and LePage, Y. (1981) Maps of electrostatic properties from X-ray data for SiO_2 (s) and Al_2O_3 (s). 12th International Congress of Crystallography, Ottawa, Canada.

Stewart, R. F. and Spackman, M. A. (1981) Charge density distributions. In M. O'Keeffe and A. Navrotsky, Eds., Structure and Bonding in Crystals, vol. 1, p. 279–298. Academic Press, New York.

Swanson, D. K. (1980) A Comparative Study of *Ab Initio* Generated Geometries for First and Second Row Atom Oxide Molecules with Corresponding Geometries in Solids. M.S. Thesis, Virginia Polytechnic Institute and State University, Blacksburg, Virginia.

Swanson, D. K., Meagher, E. P. and Gibbs, G. V. (1980) Calculation of tetrahedral and octahedral bond lengths for third row elements. (abstr.) EOS, 61, 409.

Takeuchi, Y. and Kudoh, Y. (1977) Hydrogen bonding and cation ordering in Magnet Cove pectolite. Zeitschrift für Kristallographie, 146, 281–292.

Tossell, J. A. (1975) The electronic structures of Mg, Al and Si in octahedral coordination with oxygen from SCF X_α MO calculations. Journal of Physics and Chemistry of Solids, 36, 1273–1280.

Tossell, J. A. and Gibbs, G. V. (1977) Molecular orbital studies of geometries and spectra of minerals and inorganic compounds. Physics and Chemistry of Minerals, 2, 21–57.

Tossell, J. A. and Gibbs, G. V. (1978) The use of molecular-orbital calculations on model systems for the prediction of bridging-bond-angle variations in siloxanes, silicates, silicon nitrides and silicon sulfides. Acta Crystallographica, A34, 463–472.

Varma, R., MacDiarmid, A. G. and Miller, J. G. (1964) The dipole moments and structures of disiloxane and methoxysilane. Inorganic Chemistry, 3, 1756–1757.

Voronkov, M. G., Yuzhelevskii, Yu. A. and Mileshkevich, V. P. (1975) The siloxane bond and its influence on the structure and physical properties of organosilicon compounds. Russian Chemical Reviews, 44, 355–372.

Manuscript received, December 23, 1981;
accepted for publication, January 4, 1982.